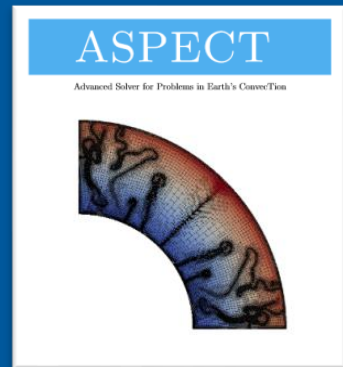
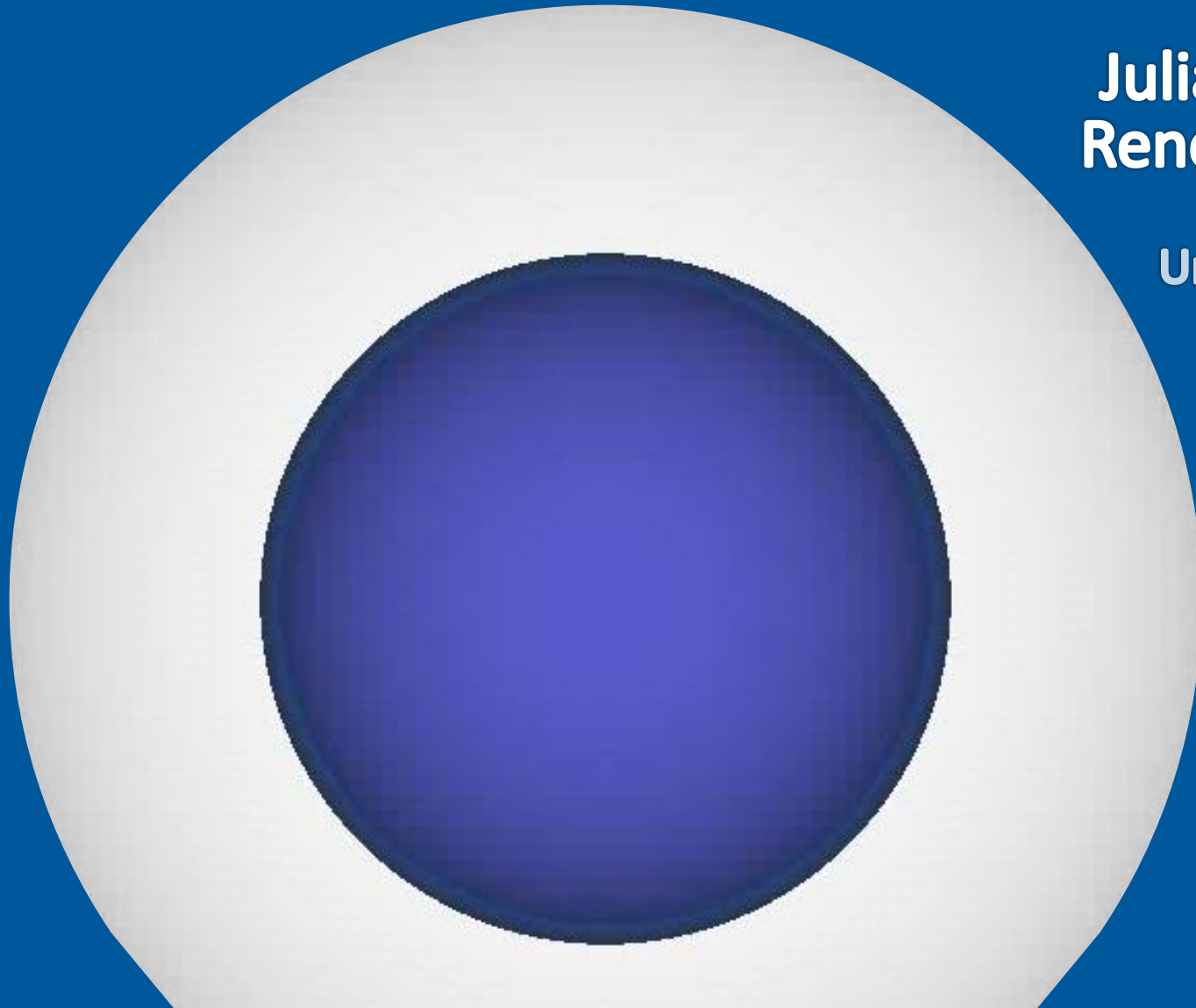


MODELLING MANTLE CONVECTION WITH CHEMICAL AND RHEOLOGICAL HETEROGENEITIES

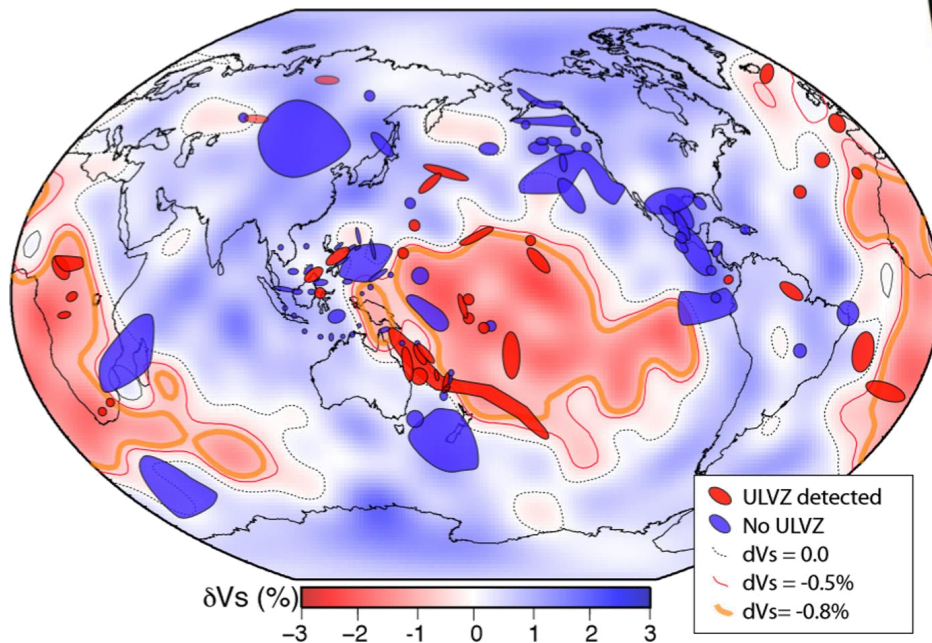
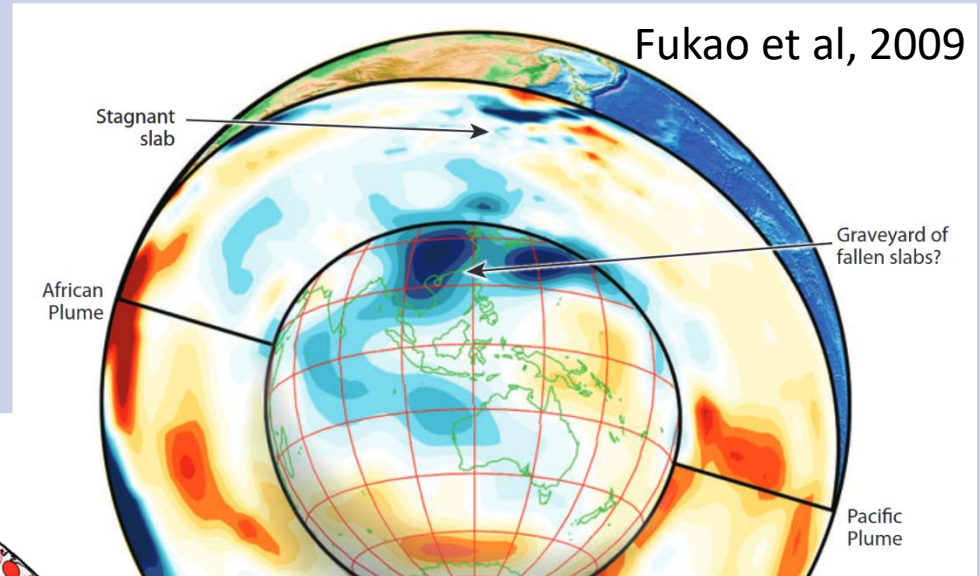
**Juliane Dannberg
Rene Gassmoeller**

**University of Florida,
University of
California, Davis**

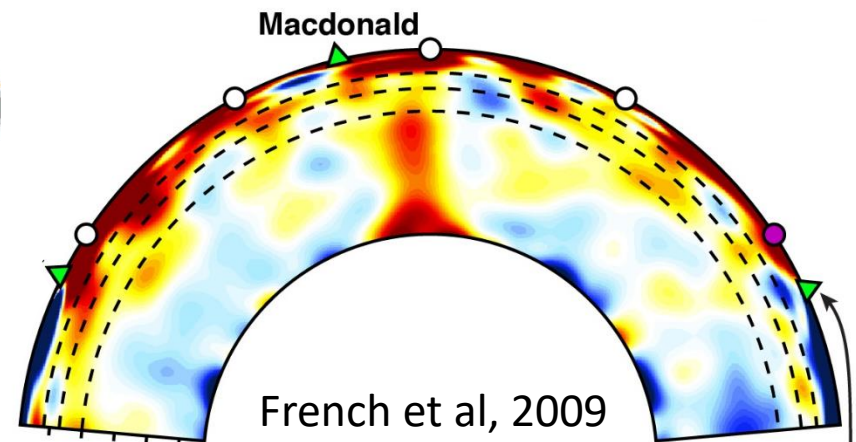


MANTLE HETEROGENEITY ABOVE THE CMB

- * LLSVPs
- * ULVZs
- * Slab graveyards?
- * Starting plumes?

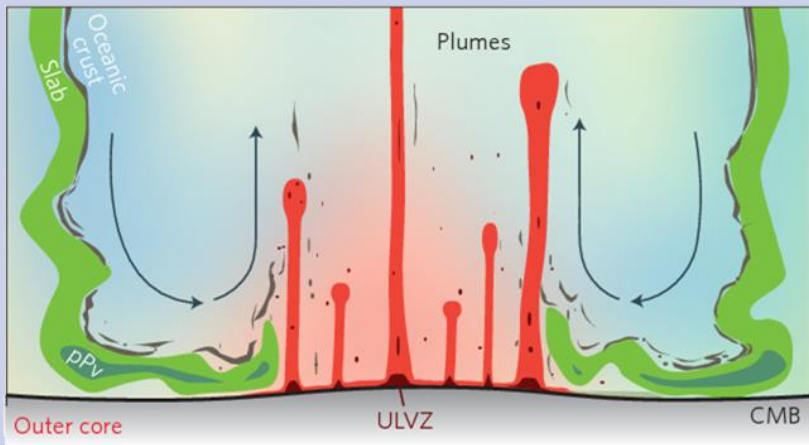


McNamara, 2019

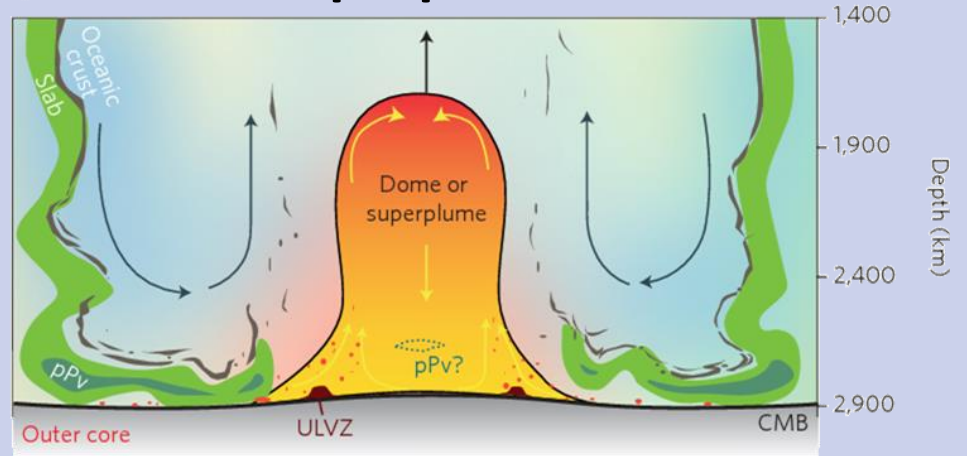


MANTLE HETEROGENEITY ABOVE THE CMB

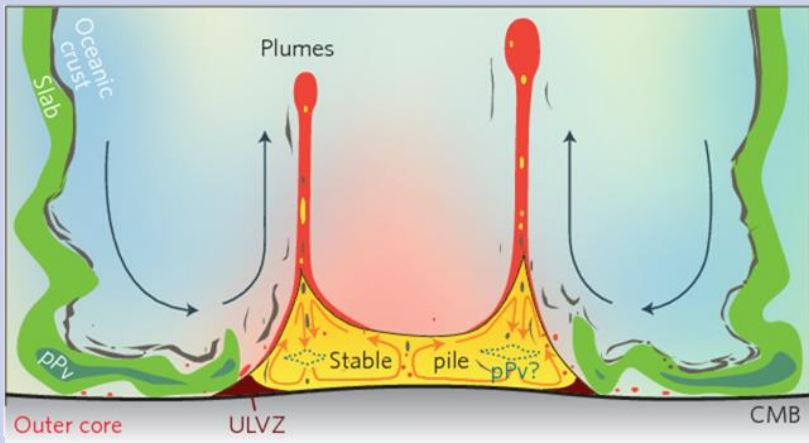
Plume cluster



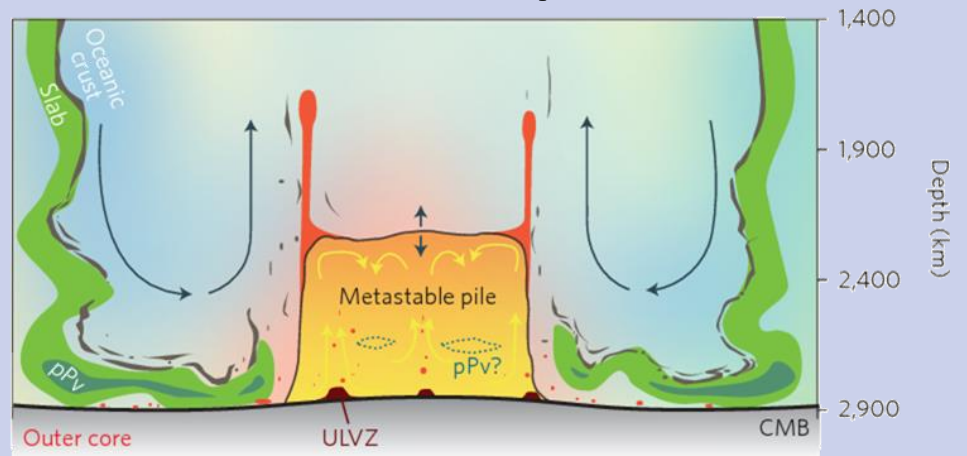
Superplume



Stable pile



Metastable pile

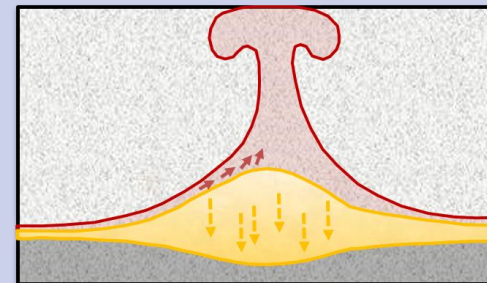
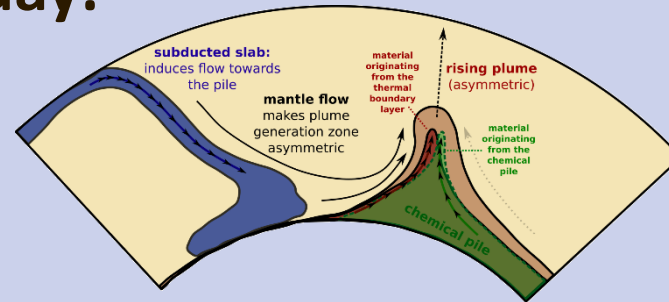


OUTLINE

* First-order effect: Thermal heterogeneities

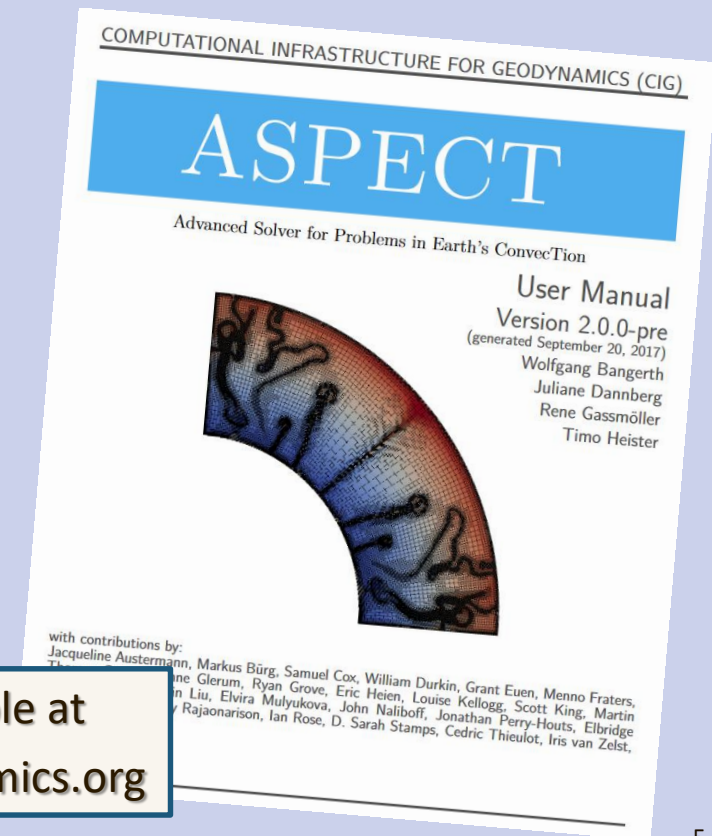
* Topics I will talk about today:

- (1) Chemical heterogeneities
- (2) Rheological heterogeneities associated with grain size variations
- (3) Heterogeneities due to melting and melt transport



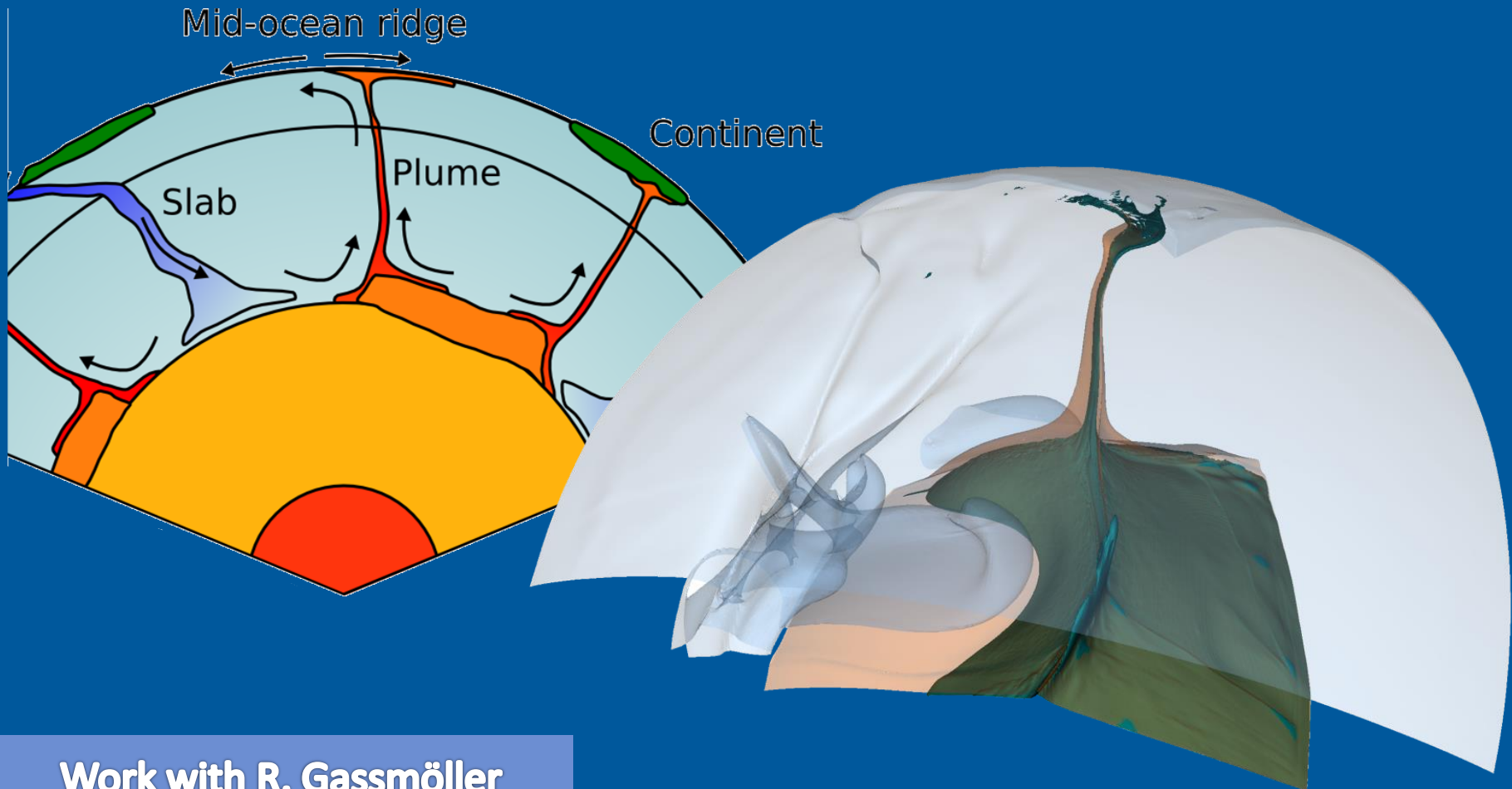
ASPECT

- ✦ Modern numerical methods:
adaptive mesh refinement, linear and nonlinear solvers,
higher-order discretizations, parallel scalability
- ✦ Usability and extensibility:
manual: 450+ pages,
40+ cookbooks/examples,
plugin architecture
- ✦ Community software
open source and developed in
the open, tested foundation,
45+ contributors



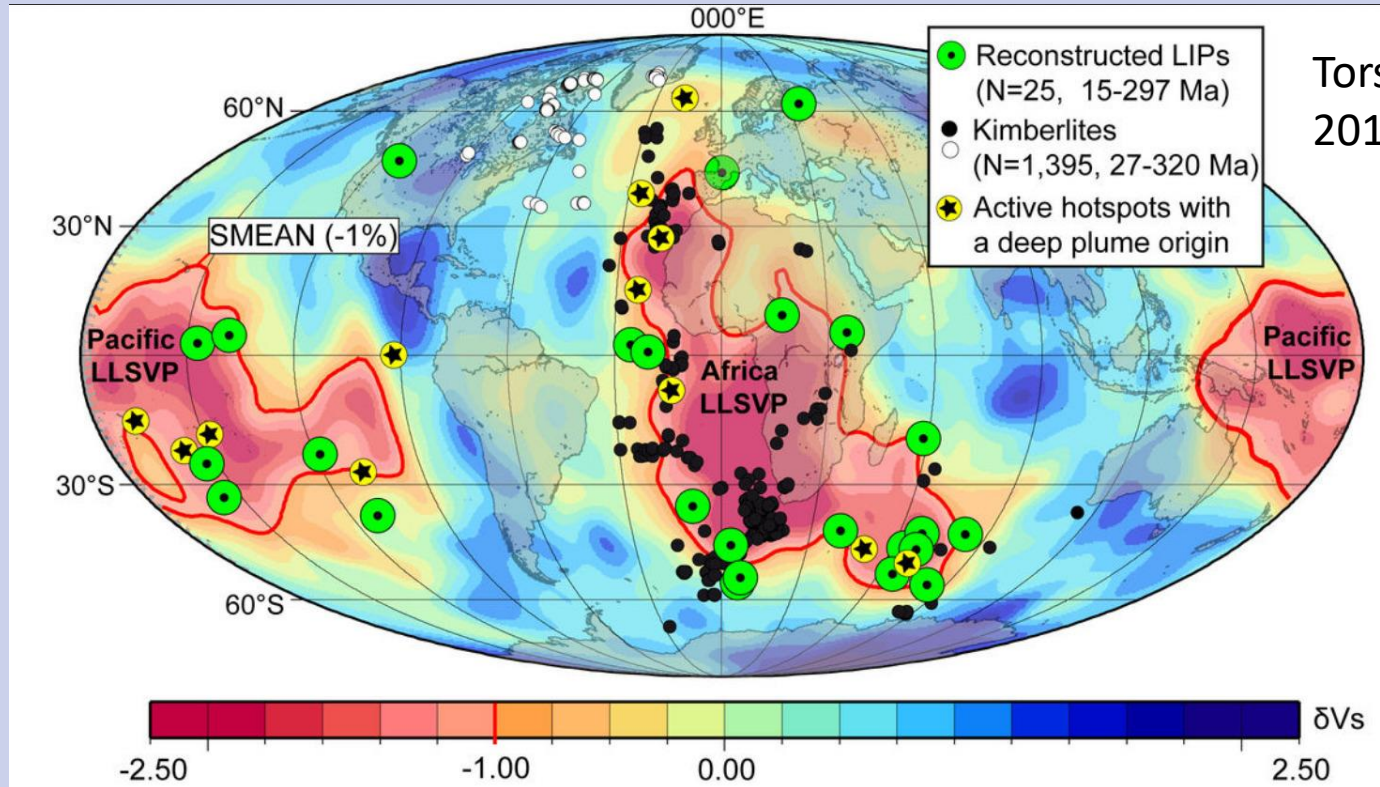
Freely available at
aspect.geodynamics.org

CHEMICAL HETEROGENEITIES: SUBDUCTED SLABS, THERMO-CHEMICAL PILES, PLUME GENERATION ZONES



Work with R. Gassmüller

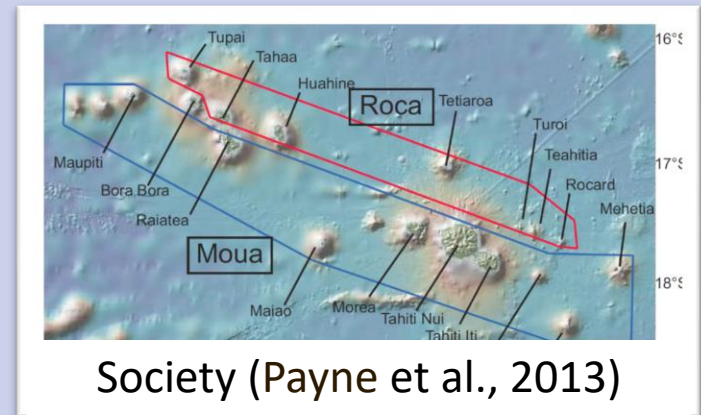
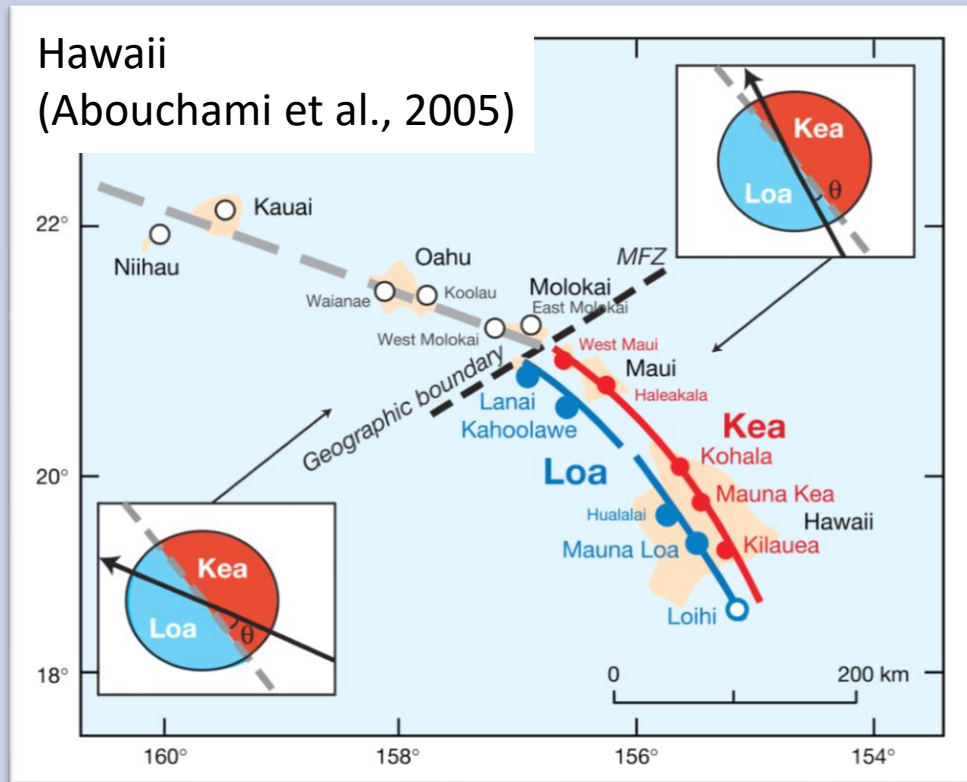
PLUME GENERATION ZONES



Torsvik et al.,
2010

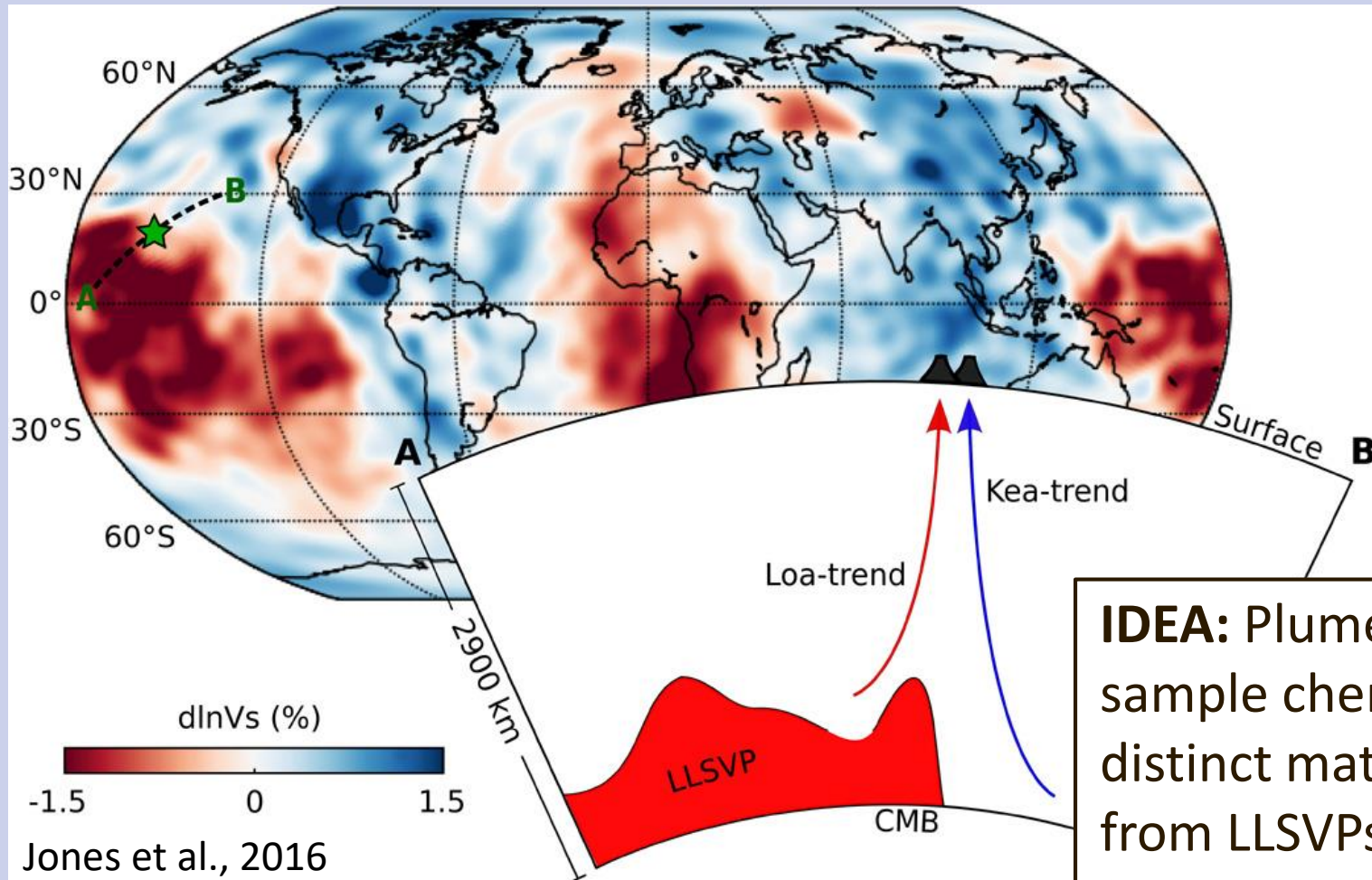
- * Many oceanic islands lie at the edges of LLSVPs when projected down to the core-mantle boundary (Thorne et al., 2004, Torsvik et al., 2006)

CHEMICAL TRENDS IN OCEAN ISLANDS



- ✳ Many oceanic islands lie at the edges of LLSVPs when projected down to the core-mantle boundary.
- ✳ Some oceanic islands display parallel volcanic chains with distinct geochemical trends.

SOURCE OF CHEMICAL ZONING

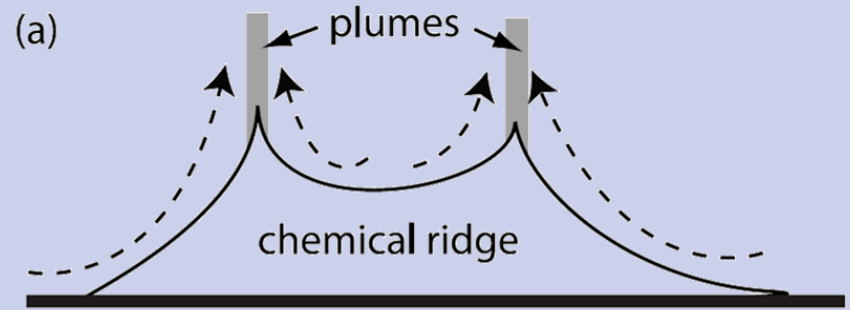


IDEA: Plumes sample chemically distinct material from LLSVPs (Weis et al, 2011)

- * Compositional boundaries of the trends in ocean islands are aligned with LLSVP outlines.

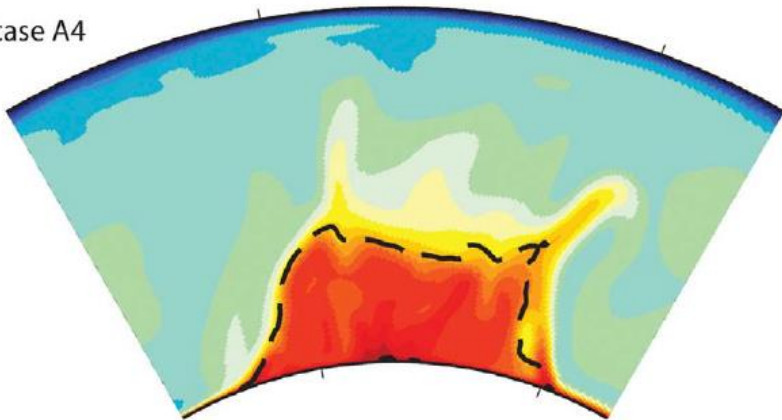
PLUMES FROM THE EDGES OF PILES

- * If dense piles have steep edges, then plumes will rise preferentially near the edges (Tan et al., 2011)



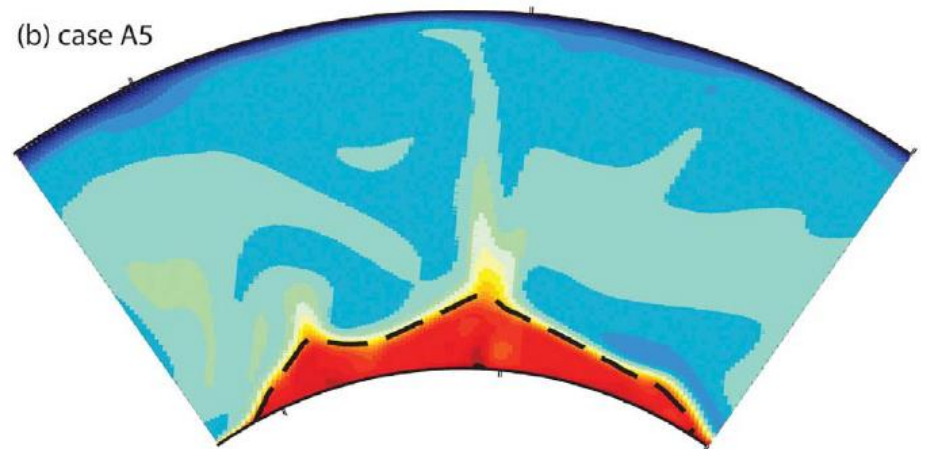
Plumes rising from the edges

(a) case A4



Plumes rising from the center

(b) case A5



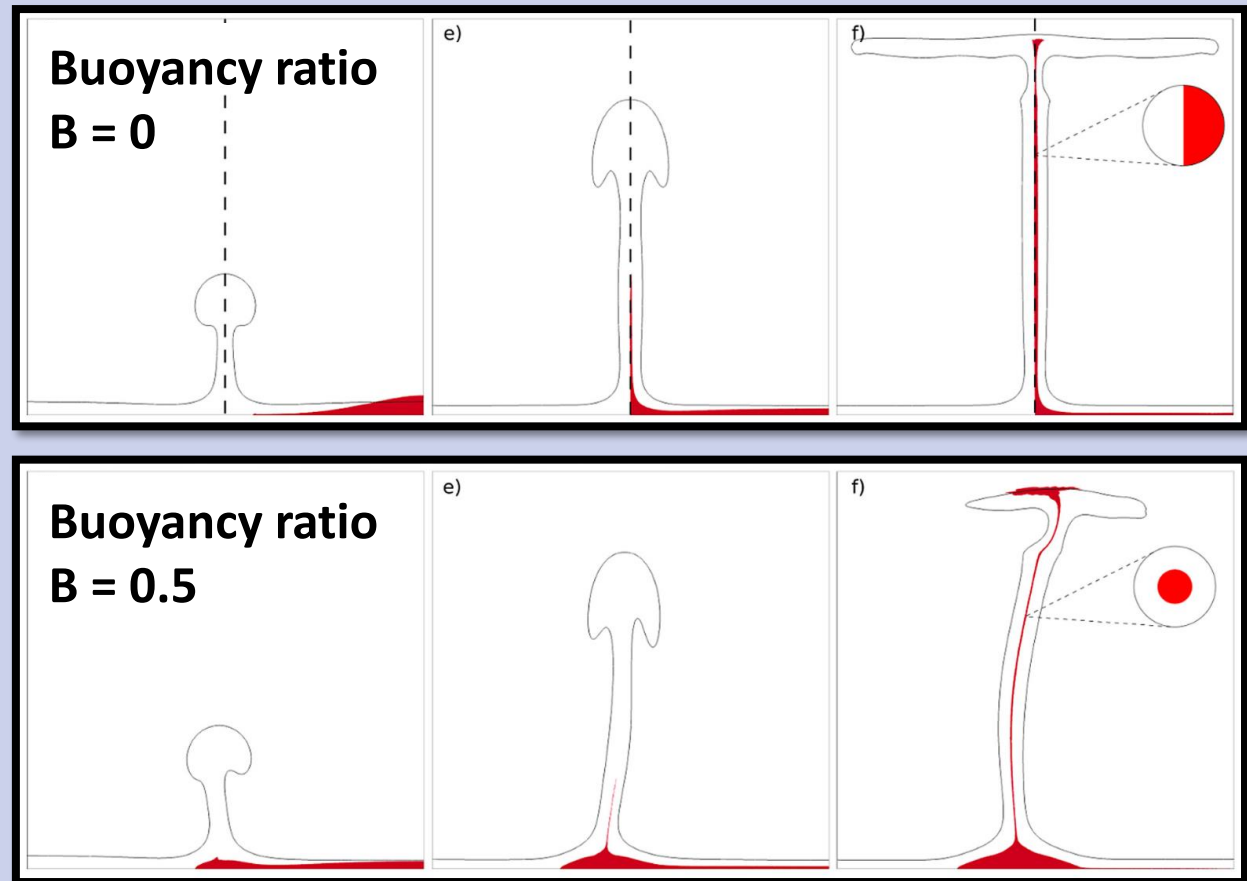
ENTRAINMENT OF A DENSE LAYER

* Buoyancy ratio:

$$B = \frac{\Delta\rho c}{\rho_0\alpha\Delta T}$$

* Problem:

Dense material is entrained symmetrically, starting at low density contrasts.



From Jones et al., 2016

QUESTIONS



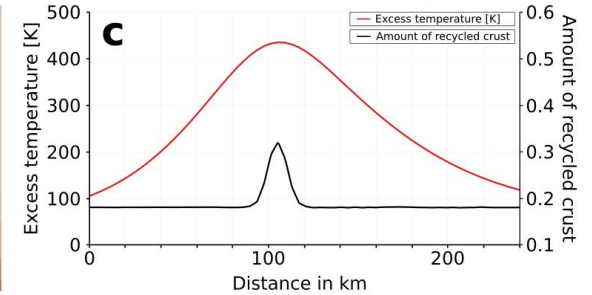
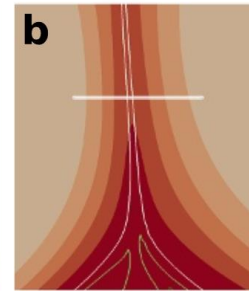
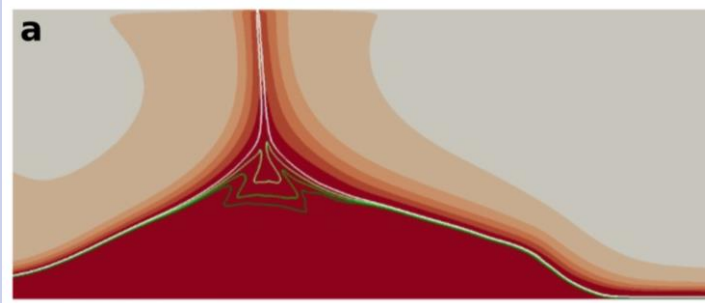
- ✳ How does bilateral chemical zoning develop in mantle plumes? (with realistic densities of entrained material)
- Hypothesis: Due to subducted slabs pushing material against the LLSVPs in the lowermost mantle
- Validation by computational models needed!

- ✳ Under which conditions is this zonation preserved and visible in melt compositions?

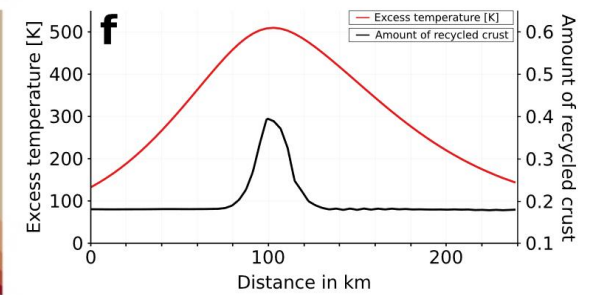
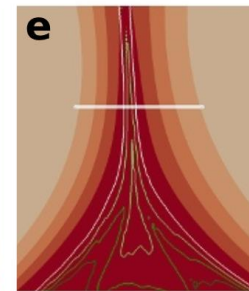
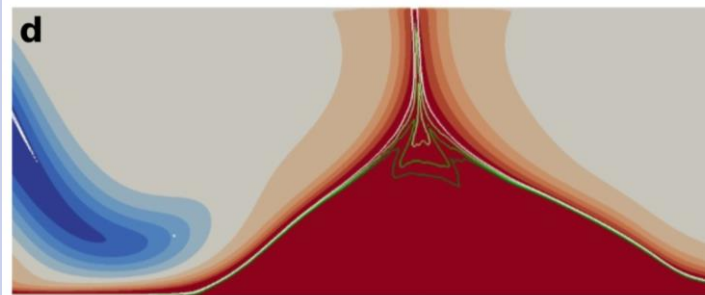
- ✳ How can geochemical observations at the surface be linked to the structure of the deep mantle?

SIMPLE 2D EXPERIMENTS

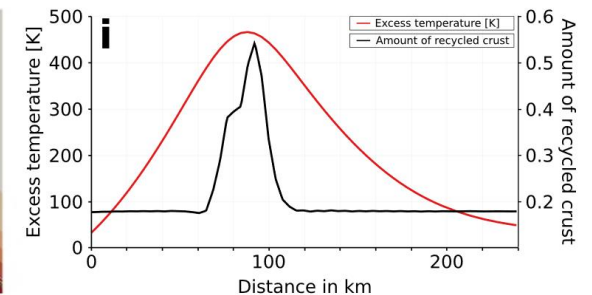
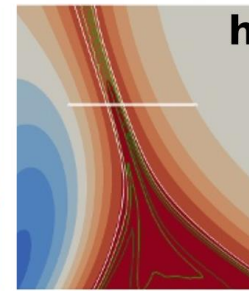
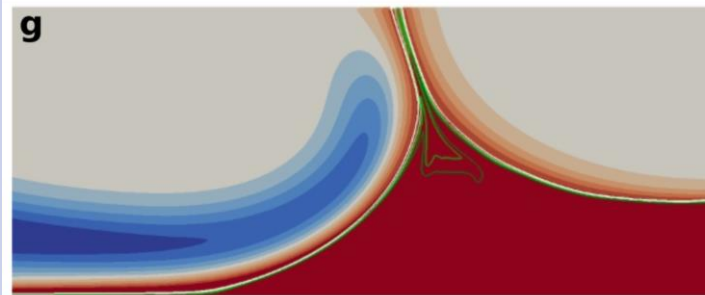
0.1 mm/yr



5 mm/yr



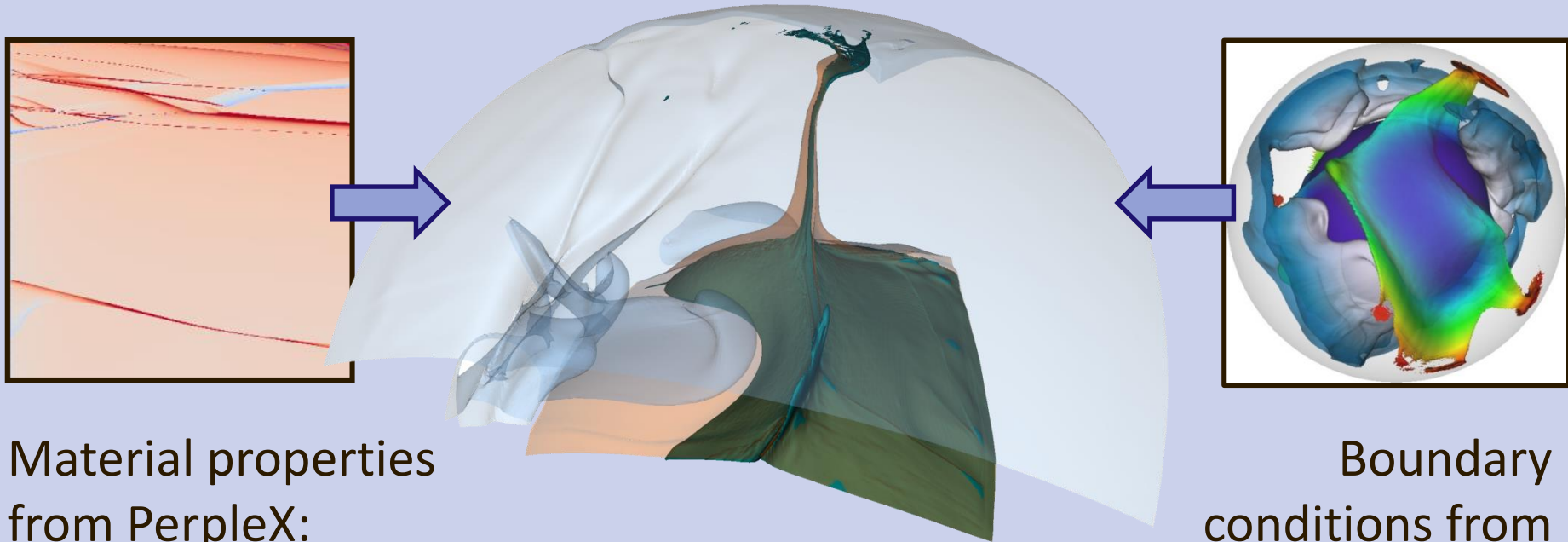
15 mm/yr



- * Subducted slabs moving towards the dense piles can make the plume generation zones asymmetric!

MORE REALISTIC MODEL SETUP

- * 3d regional convection models with ASPECT
- * Adaptive mesh, max. resolution of 10 km



Material properties
from PerpleX:

Pile: recycled oceanic crust (100%)

Mantle: harzburgite (82%)

+ recycled oceanic crust (18%)

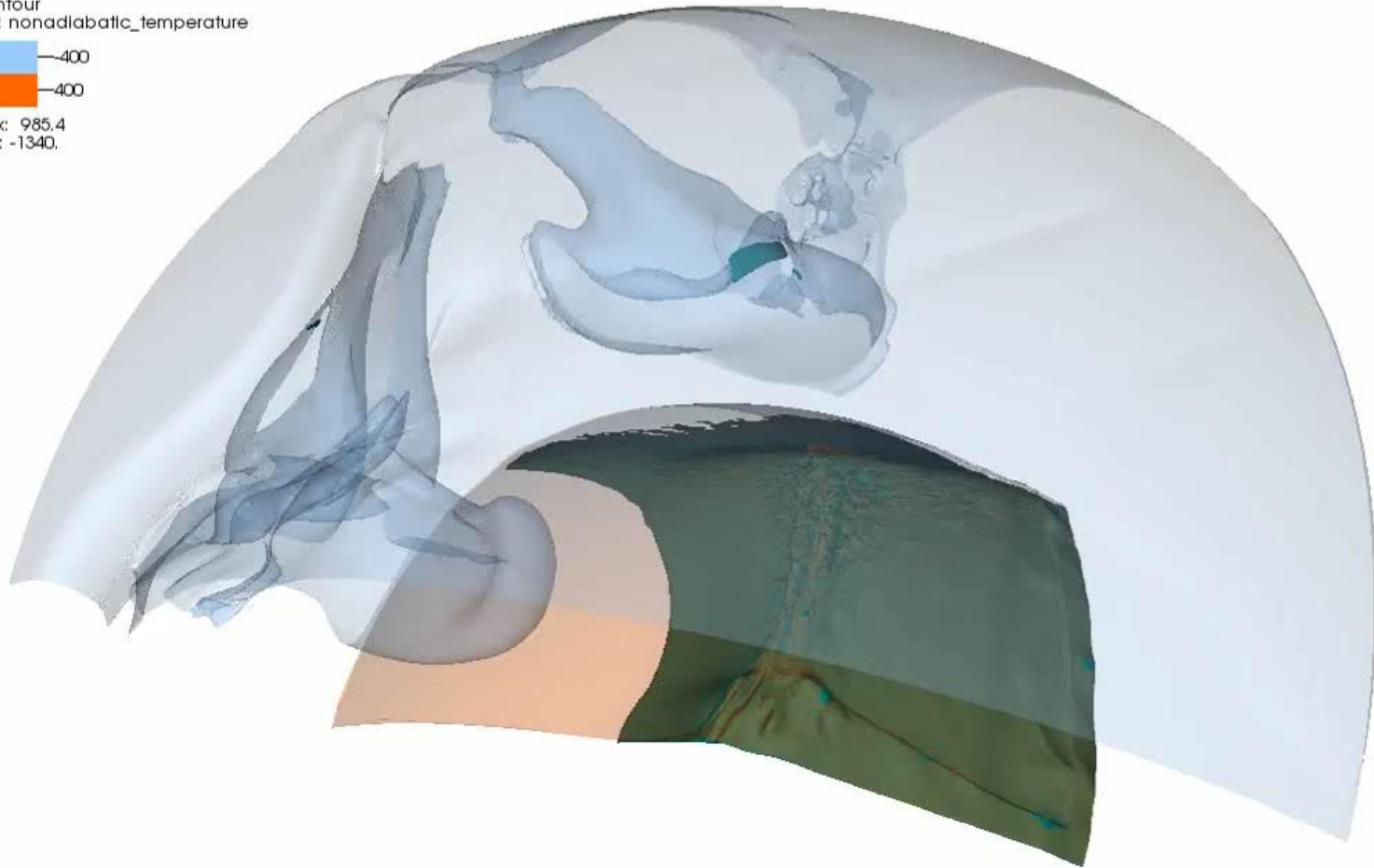
Boundary
conditions from
global model, employing
plate reconstructions for
the last 250 Myr₁₄



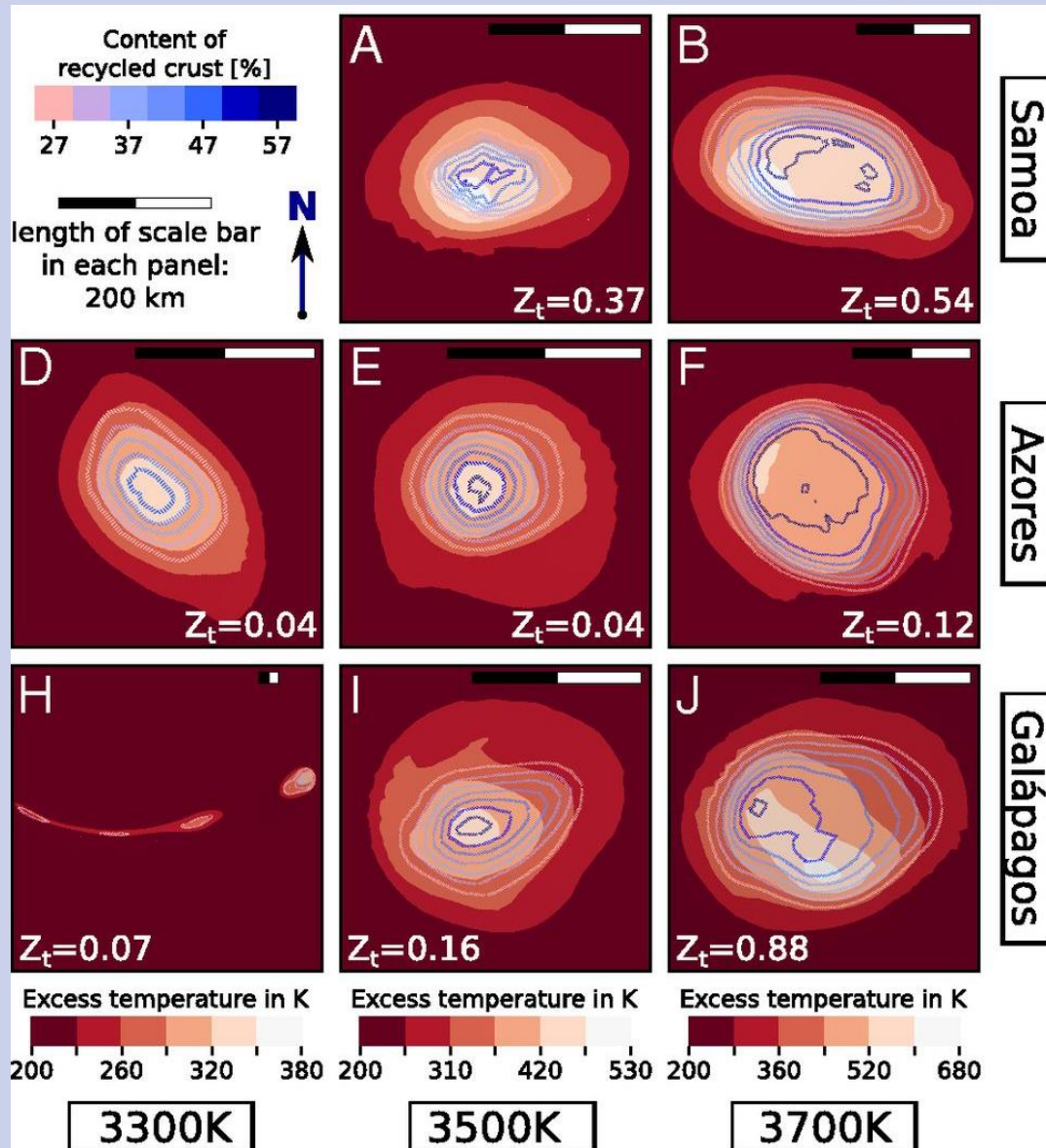
Time = 0...250 Ma

Contour
Var: MORB
0.4200
Max: 1.009
Min: 0.007082

Contour
Var: nonadiabatic_temperature
400
400
Max: 985.4
Min: -1340.

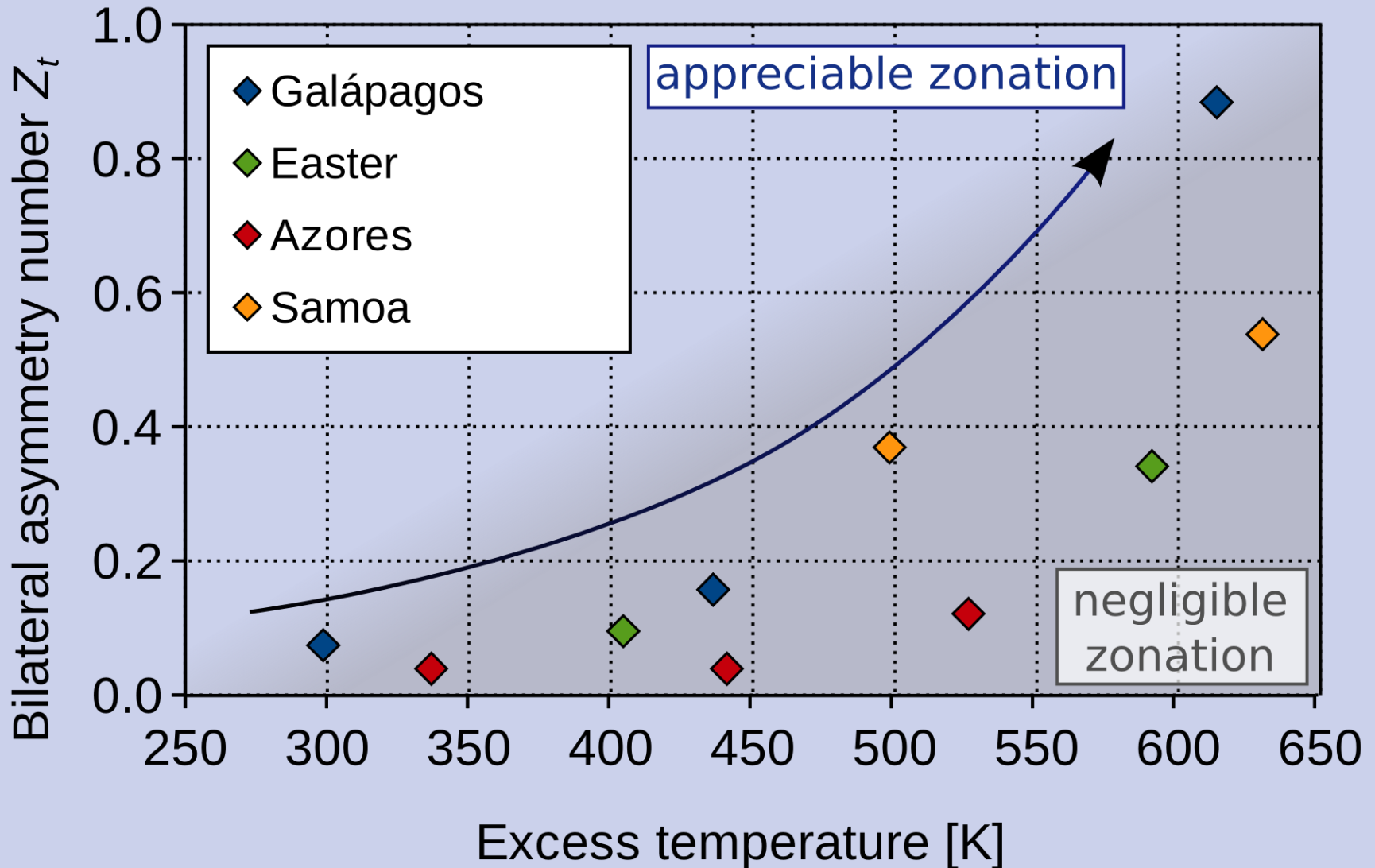


QUANTIFYING BILATERAL ZONING

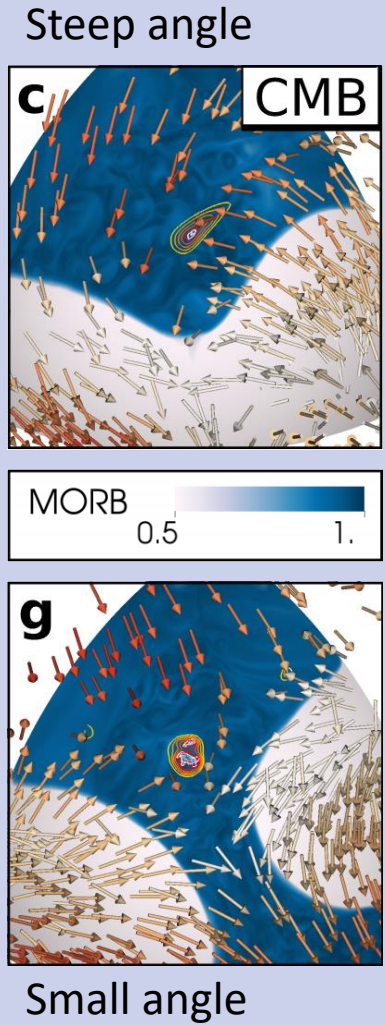
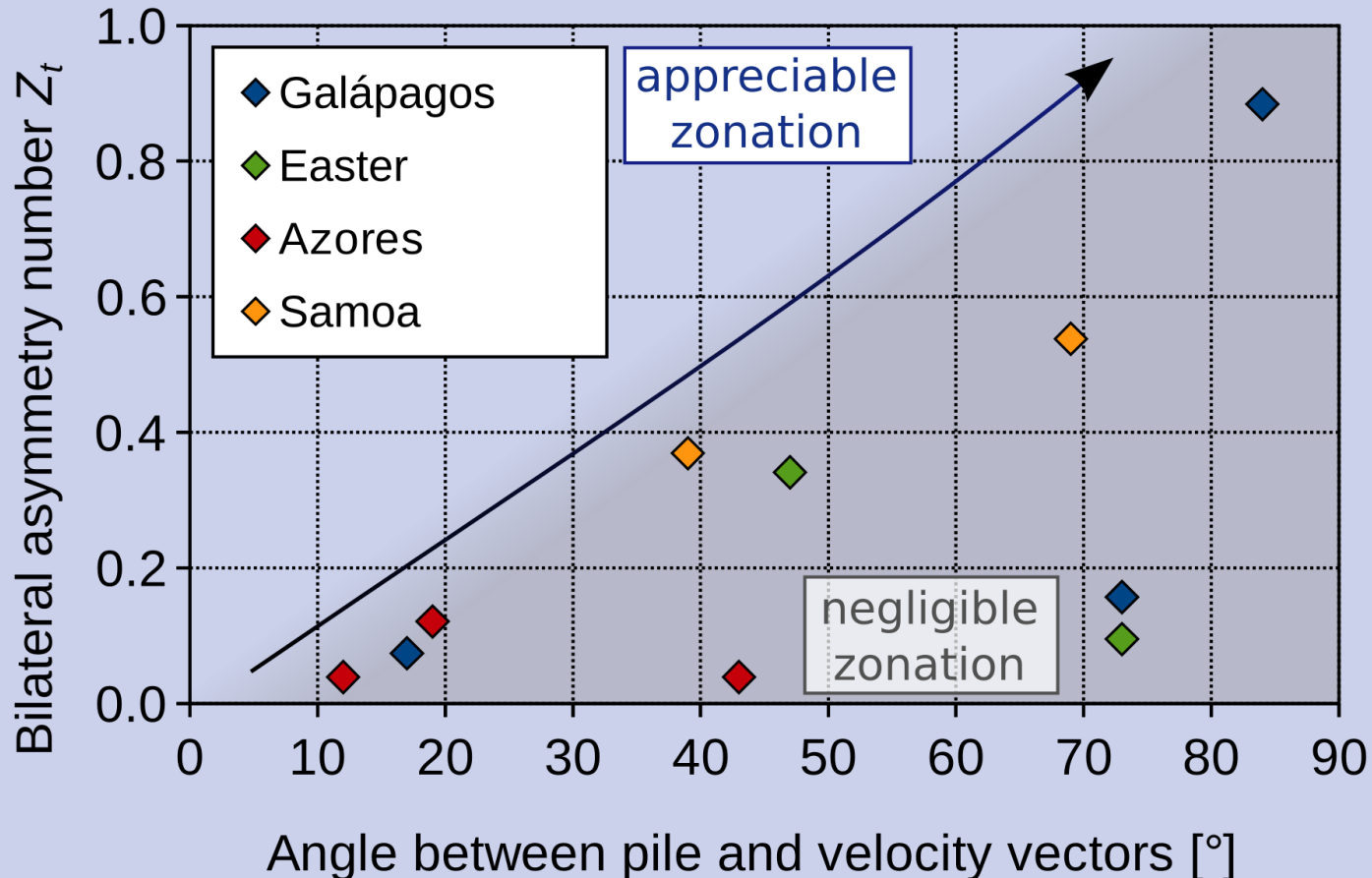


- * Slices through the plume tail at 500 km depth
- * Overlap of regions with highest plume temperature (white areas) and highest content of recycled crust (blue contours)
- * Both bilateral and concentric zoning

ZONING: DEPENDENCE ON TEMPERATURE

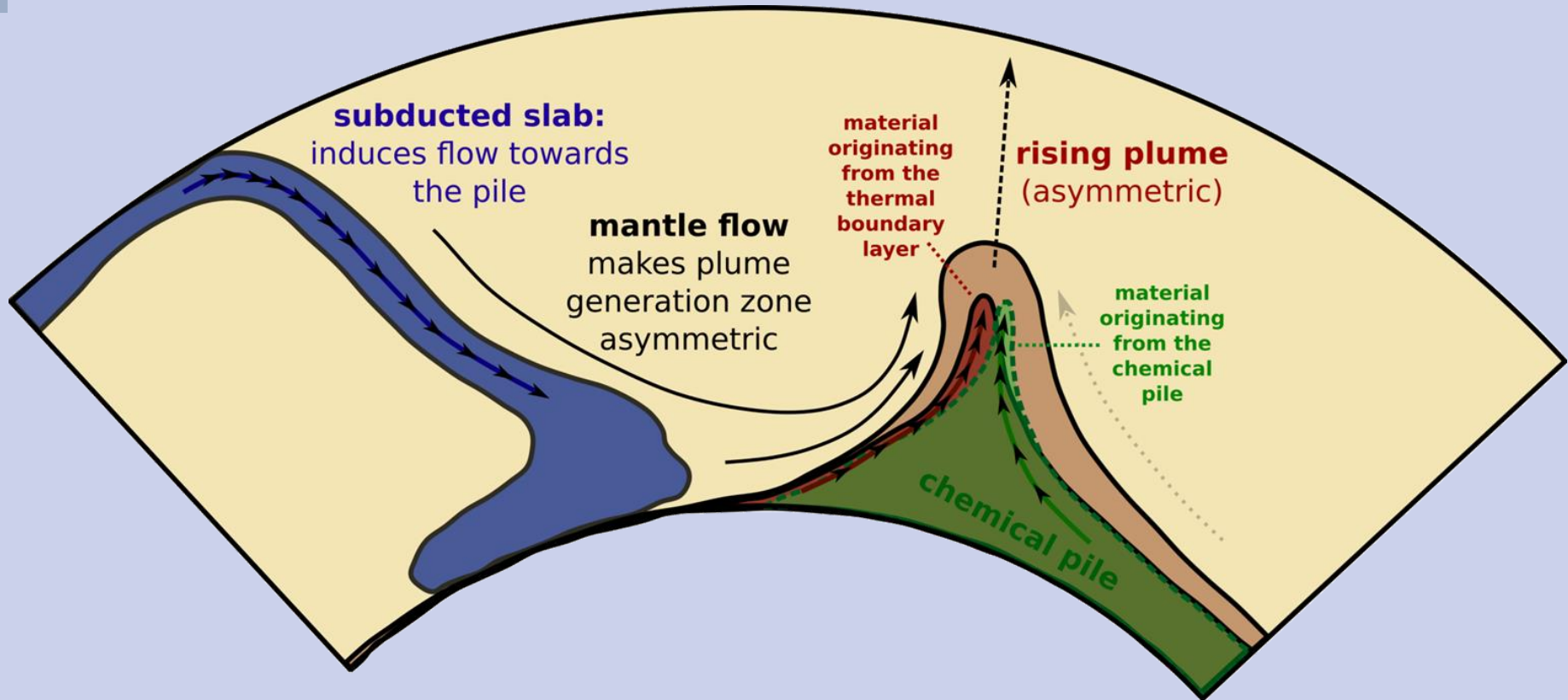


ZONING: DEPENDENCE ON ANGLE



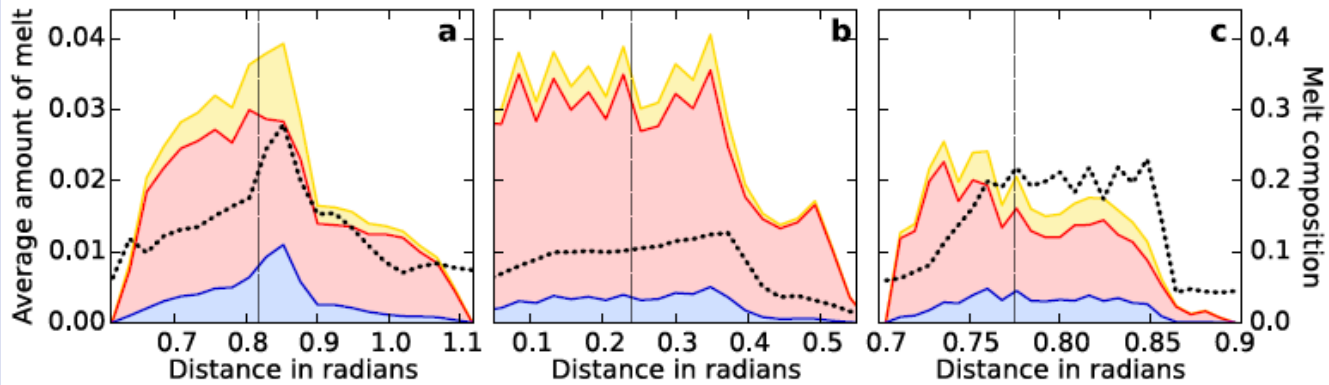
- Bilateral zonation develops only if lower mantle flow is roughly perpendicular to the edges of the piles.

DEVELOPMENT OF BILATERAL ZONING

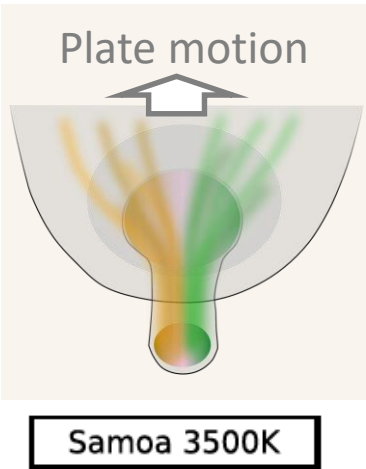
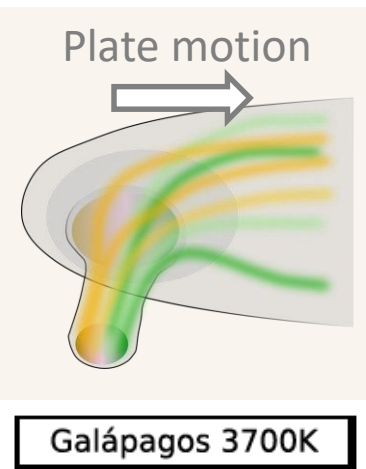
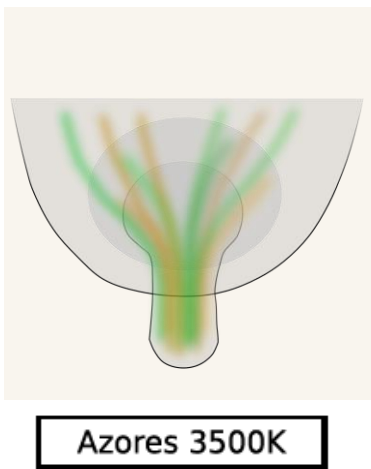


- * Pile-facing side of the plume preferentially samples material originating from the pile.
- * The side of the plume facing away from the pile preferentially samples material originating from the thermal boundary layer.

ZONING OF GENERATED MELT



<p>Concentric plume tail</p> <p>Bilateral symmetry of melt composition</p>	<p>Bilaterally zoned tail</p> <p>Plate velocity zoning</p> <p>Bilateral symmetry of melt composition</p>	<p>Bilaterally zoned tail</p> <p>Plate velocity \perp zoning</p> <p>Bilateral asymmetry of melt composition</p>
---	--	---

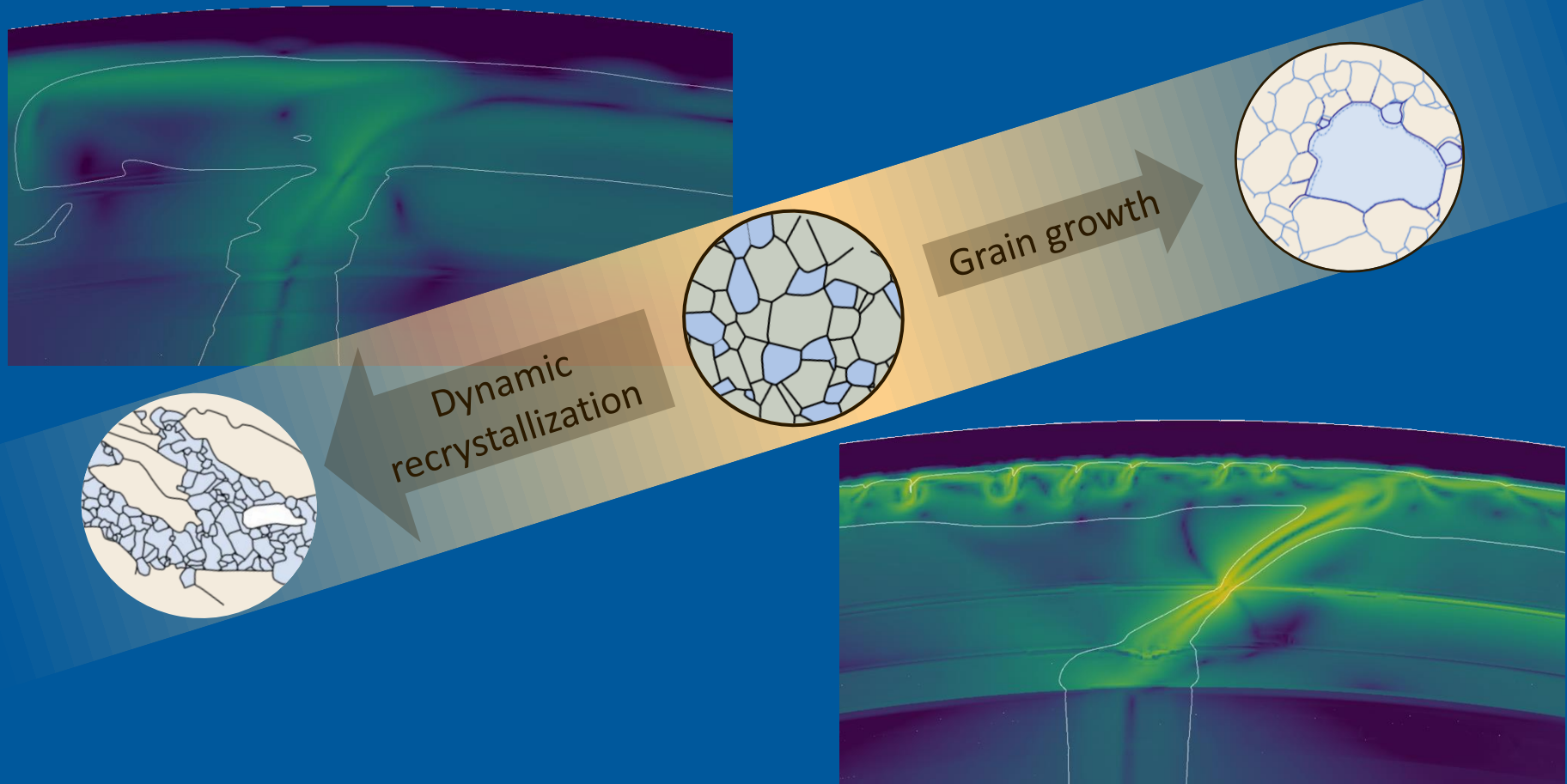


CONCLUSIONS



- * The (edges of) LLSVPs seem to be plume generation zones
- * The asymmetry of chemical trends in ocean islands could originate from the LLSVPS, if:
 - LLSVPs are chemical reservoirs containing dense material
 - Subducted slabs arriving at the core-mantle boundary cause plumes to rise from the edges of these reservoirs
 - Plume temperatures are high so they can entrain dense material asymmetrically
- * Zoning is reflected in the composition of volcanic islands if the overlying plate moves roughly perpendicular to the chemical gradient in the plume conduit.

RHEOLOGICAL HETEROGENEITIES: THE IMPORTANCE OF GRAIN SIZE EVOLUTION

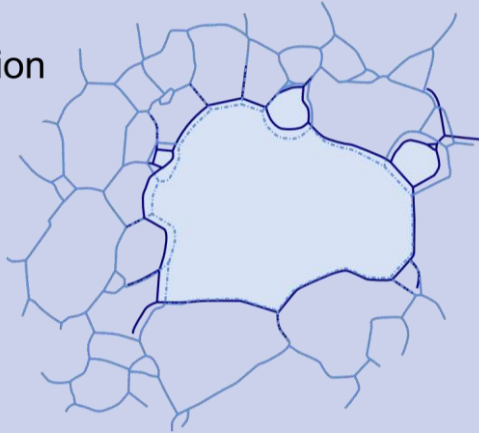


Work with Z. Eilon, U. Faul, R. Gassmüller, P. Moulik, R. Myhill

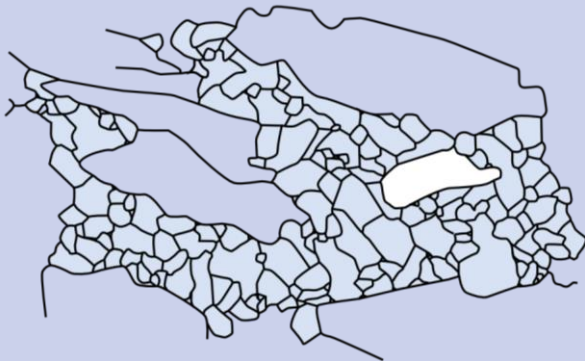
GRAIN SIZE EVOLUTION

Deformation

Grain growth:
Ripening by diffusion

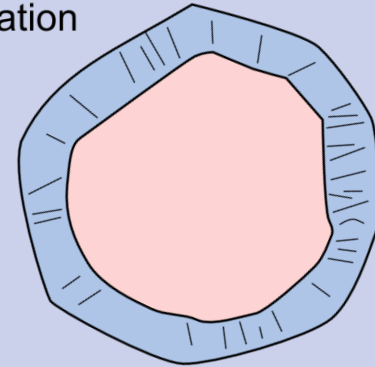


Grain size reduction:
Dynamic recrystallisation

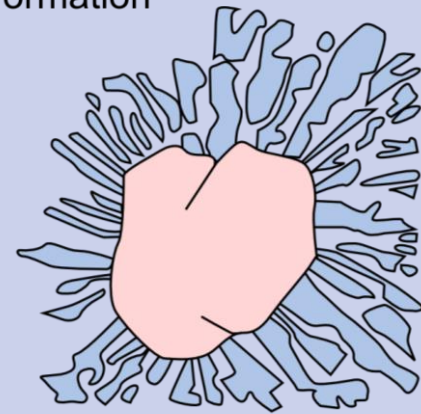


Reaction

Polymorphism:
Coherent nucleation



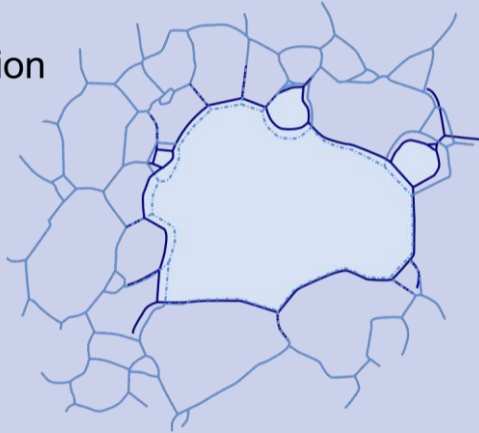
Decomposition:
Symplectite formation



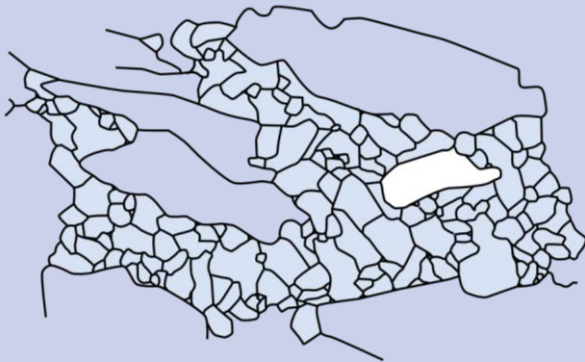
GRAIN SIZE EVOLUTION

Deformation

Grain growth:
Ripening by diffusion

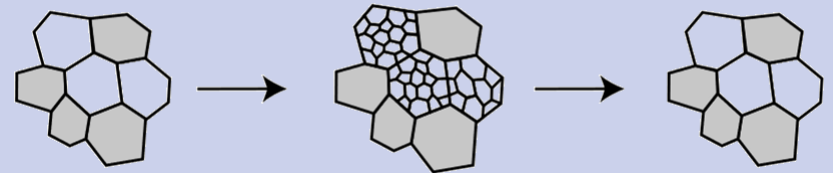


Grain size reduction:
Dynamic recrystallisation



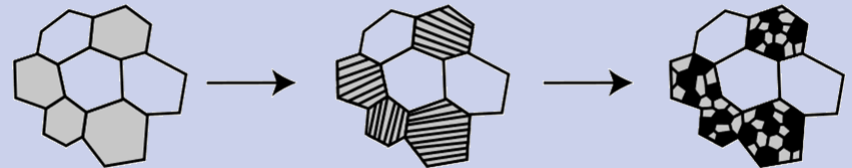
Reaction

Polymorphism:
Coherent nucleation



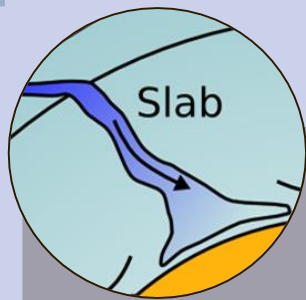
Solomatov and Reese, 2008

Decomposition:
Symplectite formation



Solomatov and Reese, 2008

GRAIN SIZE AND PHASE TRANSITIONS



Pyroxenes are dissolved in majorite garnet

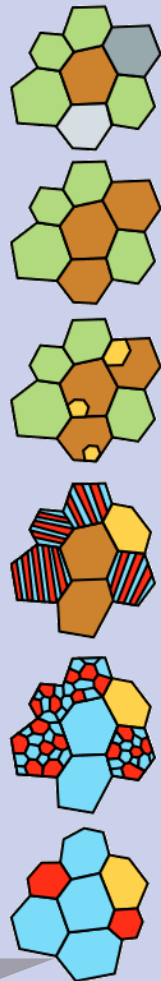
Ca-perovskite precipitates from majorite garnet

Spinel breaks down into Mg-perovskite and magnesiowüstite

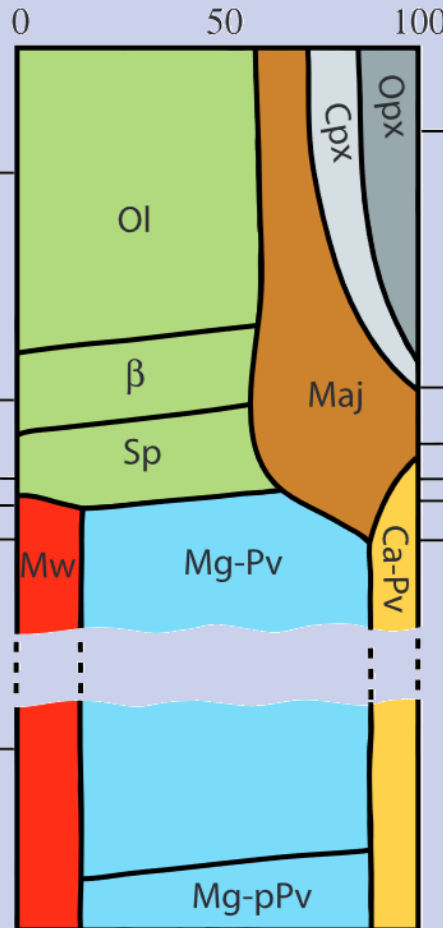
Majorite garnet is transformed to Mg-perovskite and Ca-perovskite

Ostwald ripening

Downwelling

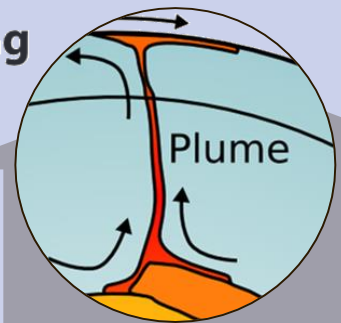


Volume fraction



Solomatov and Reese, 2008

Upwelling



Pyroxenes precipitate from majorite garnet

Ca-perovskite is out

Mg-perovskite and magnesiowüstite are out

Mg-perovskite and magnesiowüstite react and produce spinel

Mg-perovskite and Ca-perovskite transform to majorite garnet

EQUATIONS: STOKES, ENERGY BALANCE

$$-\nabla \cdot (2\eta \dot{\epsilon}_\kappa(\mathbf{u})) + \nabla p = \rho \mathbf{g},$$

$$\nabla \cdot (\rho \mathbf{u}) = 0,$$

$$\rho C_p \left(\frac{\partial T}{\partial t} + \mathbf{u} \cdot \nabla T \right) - \nabla \cdot k \nabla T = 2\eta \dot{\epsilon}_\kappa(\mathbf{u}) : \dot{\epsilon}_\kappa(\mathbf{u}) + \alpha T (\mathbf{u} \cdot \nabla p) + Q$$

EQUATIONS: COMPOSITE RHEOLOGY

$$-\nabla \cdot (2\eta \dot{\epsilon}_\kappa(\mathbf{u})) + \nabla p = \rho \mathbf{g},$$

$$\nabla \cdot (\rho \mathbf{u}) = 0,$$

$$\rho C_p \left(\frac{\partial T}{\partial t} + \mathbf{u} \cdot \nabla T \right) - \nabla \cdot k \nabla T = 2\eta \dot{\epsilon}_\kappa(\mathbf{u}) : \dot{\epsilon}_\kappa(\mathbf{u}) + \alpha T (\mathbf{u} \cdot \nabla p) + Q$$

$$\eta_{\text{diff}} = \frac{1}{2} A^{-\frac{1}{n}} d^{\frac{m}{n}} \exp \left(\frac{E^* + PV^*}{nRT} \right)$$

$$\eta_{\text{dis}} = \frac{1}{2} A^{-\frac{1}{n}} \dot{\epsilon}_{\text{dis,II}}^{\frac{1-n}{n}} \exp \left(\frac{E^* + PV^*}{nRT} \right)$$

$$\eta_{\text{eff}} = \frac{\eta_{\text{diff}} \eta_{\text{dis}}}{\eta_{\text{diff}} + \eta_{\text{dis}}}$$

Diffusion creep
(grain-size dependent)

Dislocation creep
(stress/strain-rate dependent)

EQUATIONS: COMPOSITE RHEOLOGY

$$-\nabla \cdot (2\underline{\eta} \dot{\epsilon}_{\kappa}(\mathbf{u})) + \nabla p = \rho \mathbf{g},$$

$$\nabla \cdot (\rho \mathbf{u}) = 0,$$

$$\rho C_p \left(\frac{\partial T}{\partial t} + \mathbf{u} \cdot \nabla T \right) - \nabla \cdot k \nabla T = 2\underline{\eta} \dot{\epsilon}_{\kappa}(\mathbf{u}) : \dot{\epsilon}_{\kappa}(\mathbf{u}) + \alpha T (\mathbf{u} \cdot \nabla p) + Q$$

$$\eta_{\text{diff}} = \frac{1}{2} A^{-\frac{1}{n}} \underline{d}^{\frac{m}{n}} \exp \left(\frac{E^* + PV^*}{nRT} \right)$$

Diffusion creep
(grain-size dependent)

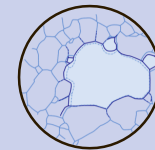
$$\eta_{\text{dis}} = \frac{1}{2} A^{-\frac{1}{n}} \dot{\epsilon}_{\text{dis,II}}^{\frac{1-n}{n}} \exp \left(\frac{E^* + PV^*}{nRT} \right)$$

Dislocation creep
(stress/strain-rate dependent)

$$\eta_{\text{eff}} = \frac{\eta_{\text{diff}} \eta_{\text{dis}}}{\eta_{\text{diff}} + \eta_{\text{dis}}}$$

Grain size evolution

$$\left(\frac{\partial d}{\partial t} + \mathbf{u} \cdot \nabla d \right) = p_g^{-1} d^{1-p_g} k_g \exp \left(-\frac{E_g + PV_g}{RT} \right)$$



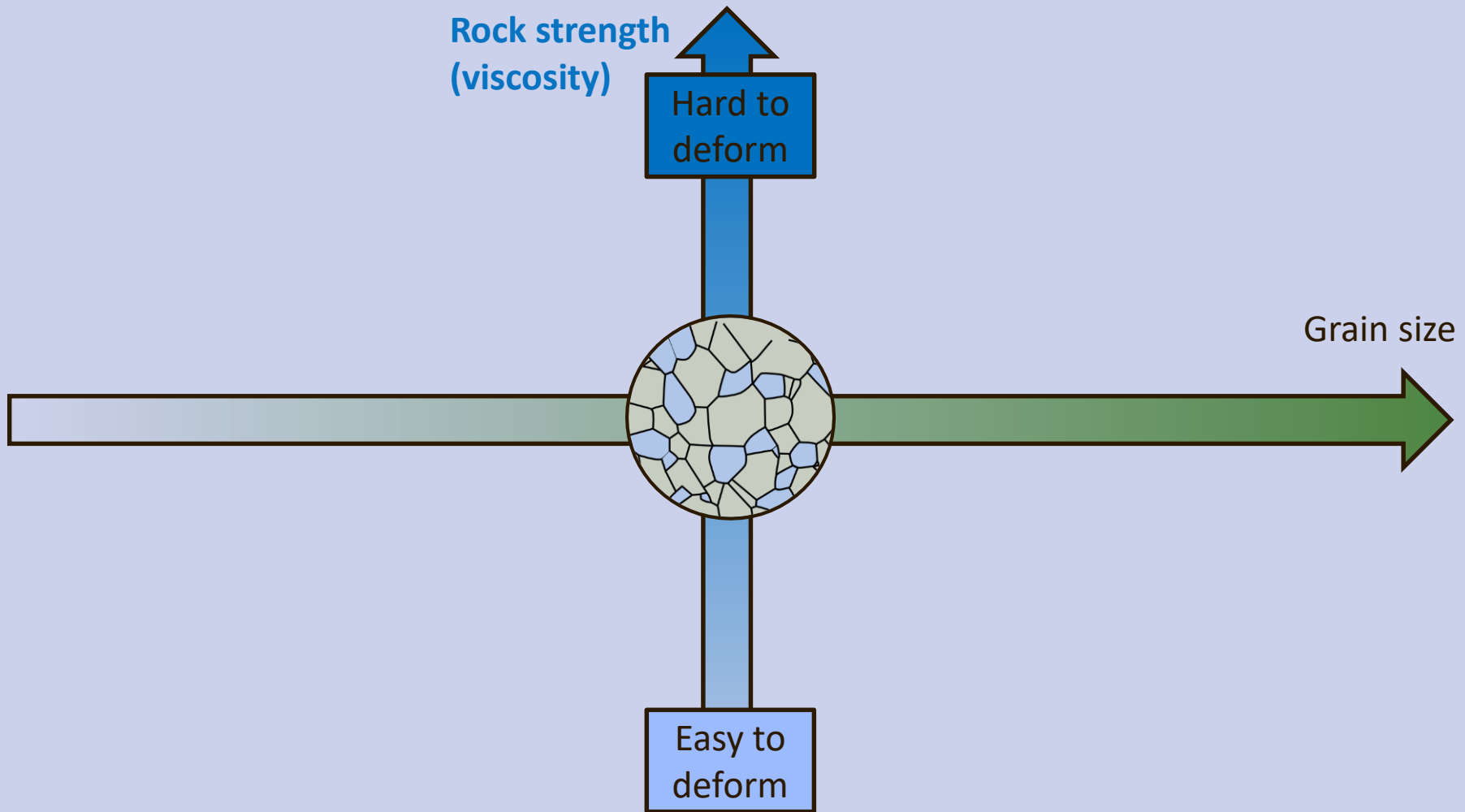
Grain growth

$$- 4 \dot{\epsilon}_{\text{II}} \dot{\epsilon}_{\text{dis}} \eta_{\text{eff}} \frac{\lambda d^2}{c\gamma},$$



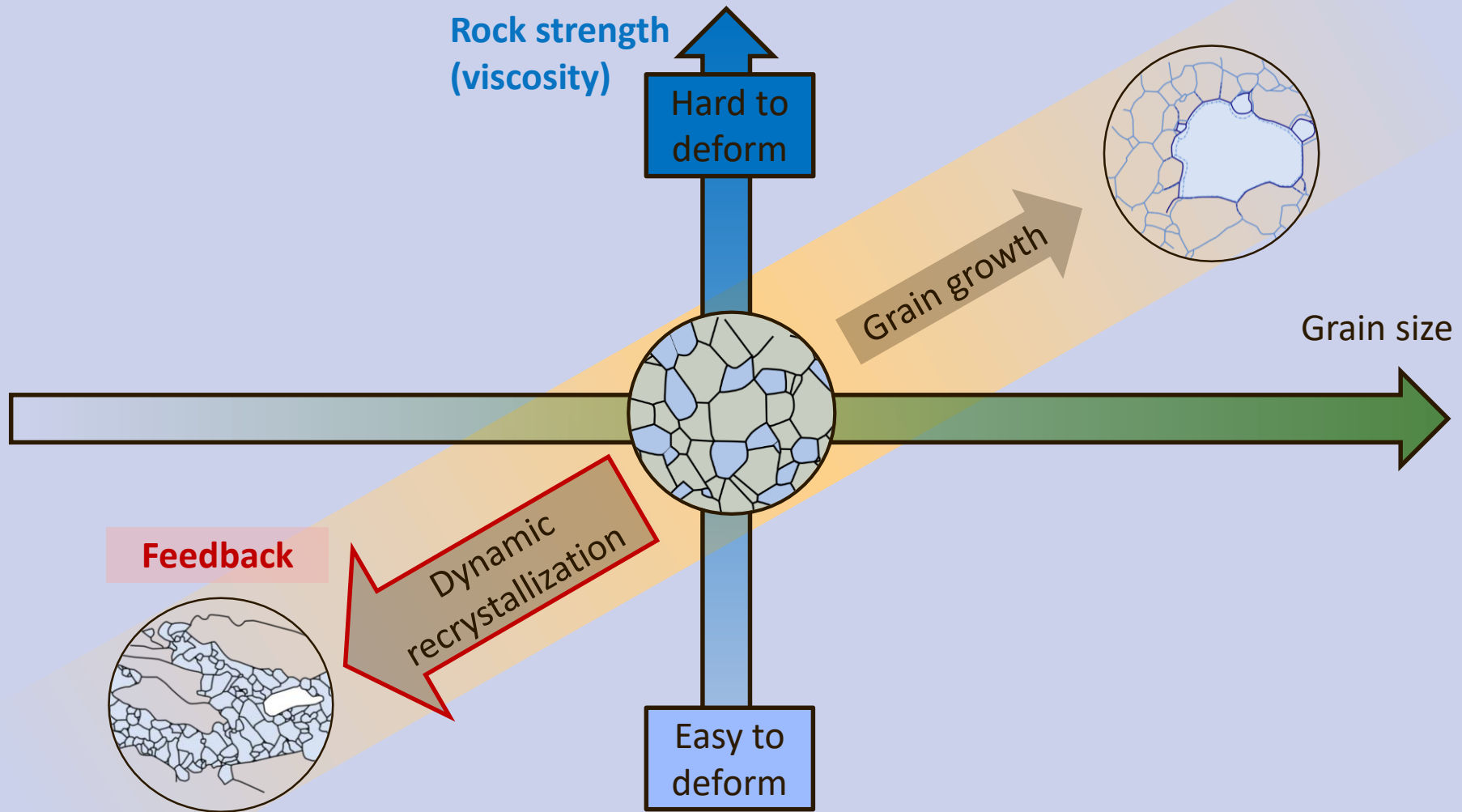
Grain size reduction

HOW GRAIN SIZE AFFECTS DEFORMATION



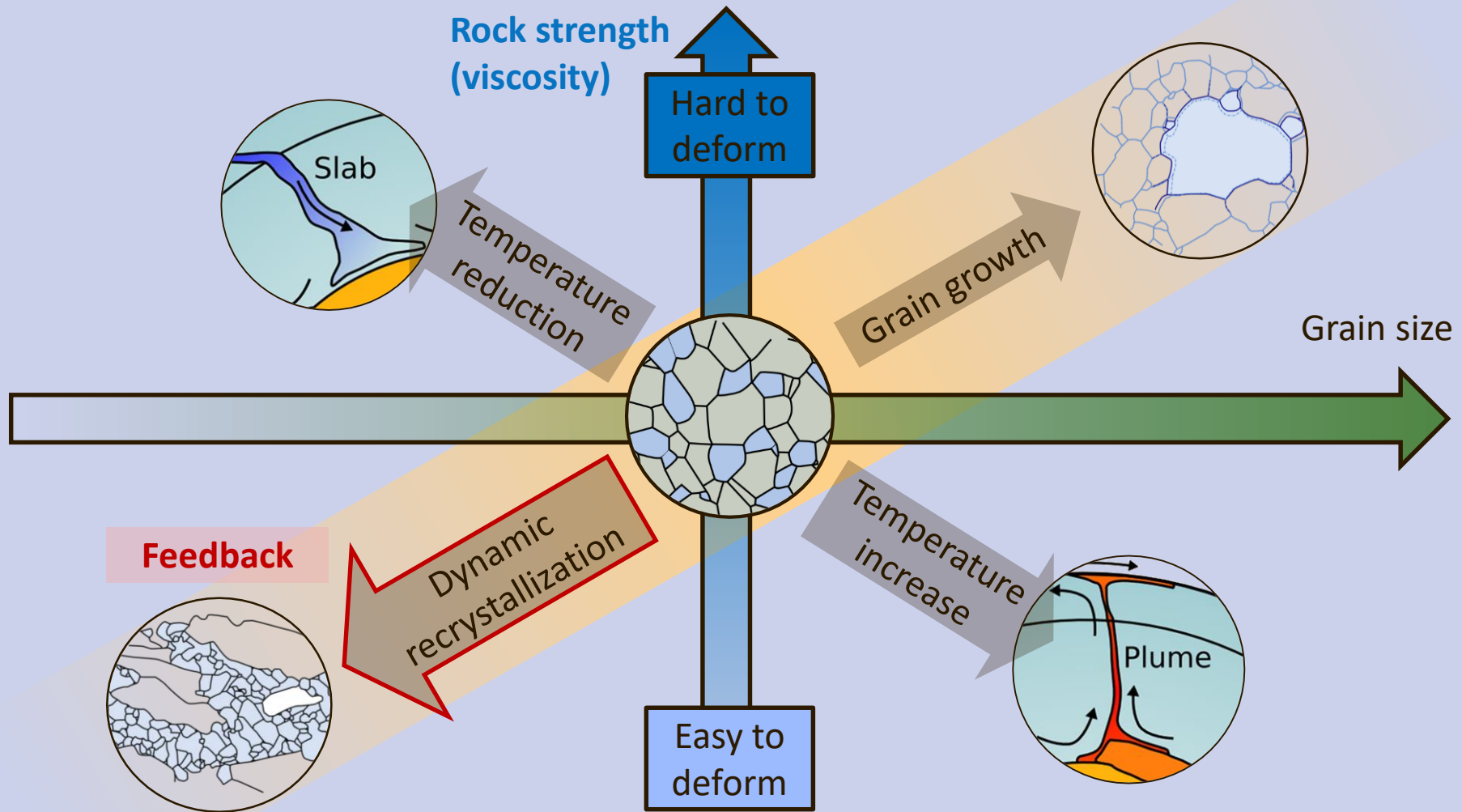
See also: **Dannberg, J., Eilon, Z., Faul, U., Gassmüller, R., Moulik, P., & Myhill, R. (2017).** The importance of grain size to mantle dynamics and seismological observations. *Geochemistry, Geophysics, Geosystems*, 18(8), 3034-3061.

HOW GRAIN SIZE AFFECTS DEFORMATION



See also: **Dannberg, J., Eilon, Z., Faul, U., Gassmüller, R., Moulik, P., & Myhill, R. (2017).** The importance of grain size to mantle dynamics and seismological observations. *Geochemistry, Geophysics, Geosystems*, 18(8), 3034-3061.

HOW GRAIN SIZE AFFECTS DEFORMATION

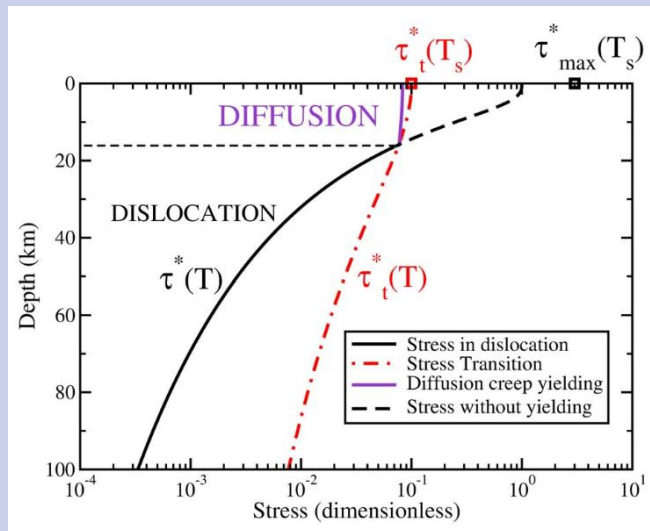


See also: **Dannberg, J., Eilon, Z., Faul, U., Gasmöller, R., Moulik, P., & Myhill, R. (2017).** The importance of grain size to mantle dynamics and seismological observations. *Geochemistry, Geophysics, Geosystems*, 18(8), 3034-3061.

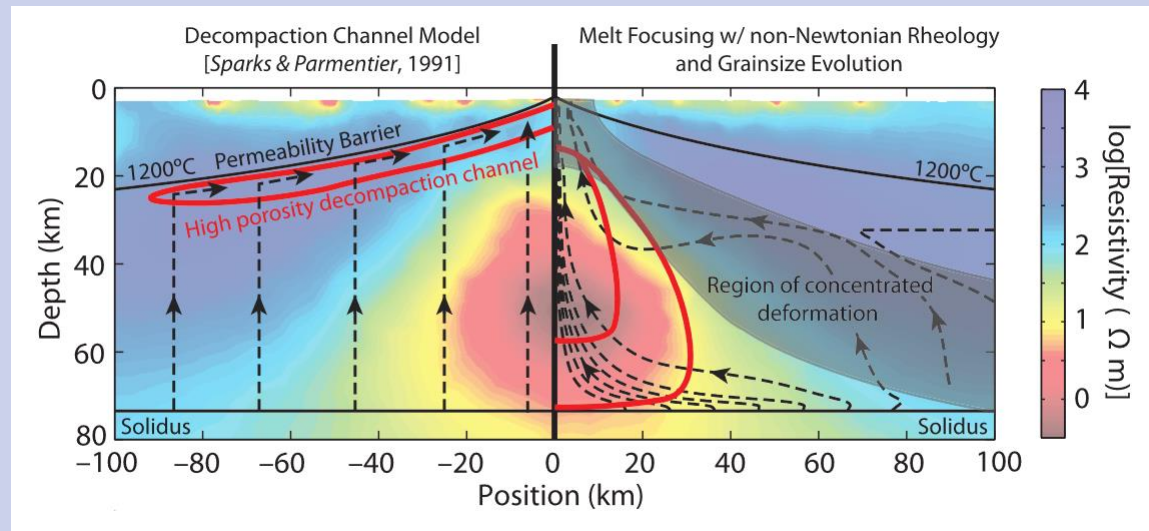
IMPORTANCE OF GRAIN SIZE

Important for:

- ✦ Convection regime of terrestrial planets (breaking the stagnant lid; Rozel 2012)
- ✦ Channeling melt to mid-ocean ridges (Turner et al., 2017)
- ✦ Collapse of passive margins (Mulyukova & Bercovici, 2018)
- ✦ Icy satellites, ...

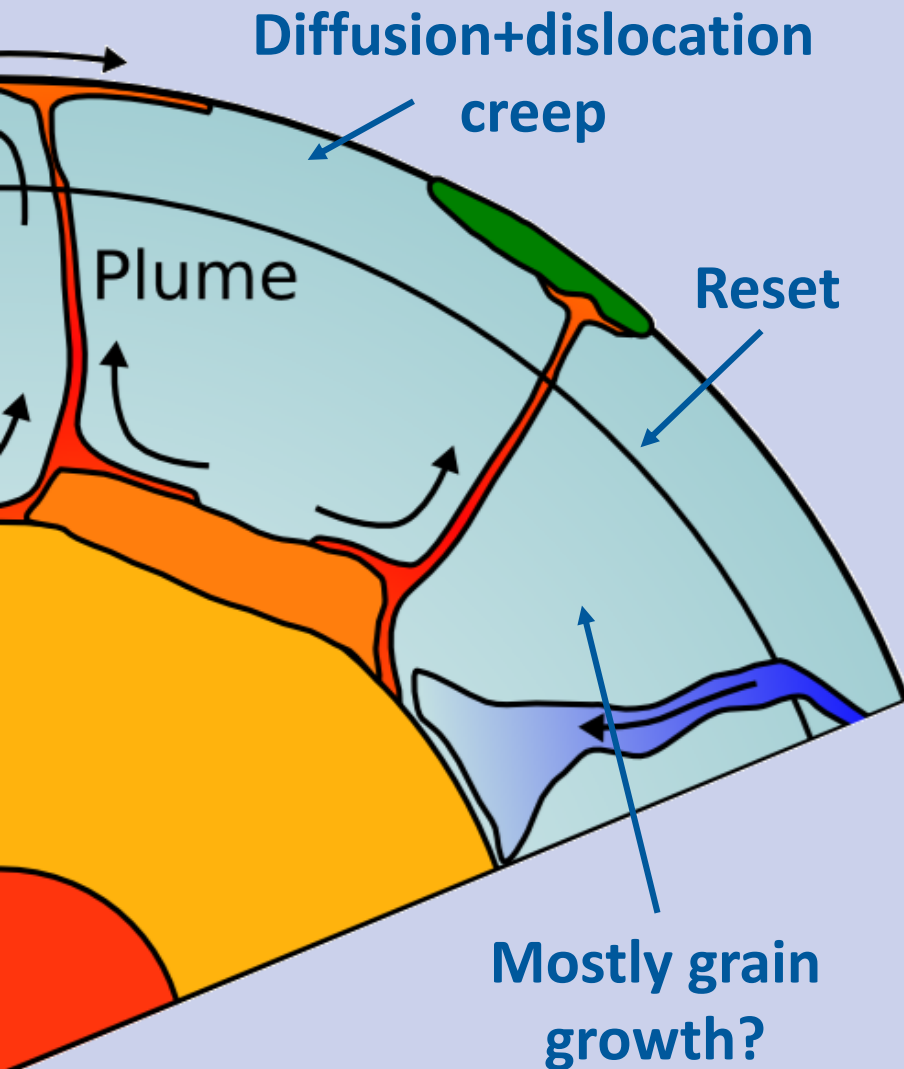


Rozel, 2012



Turner et al., 2017

GRAIN SIZE EVOLUTION IN THE MANTLE



Upper mantle:

- * Dislocation creep is dominant deformation mechanism
- * Interplay of grain growth and grain size reduction

Grain size reset

at ringwoodite \rightarrow bridgmanite + ferropericlase transition

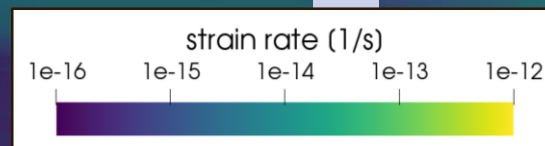
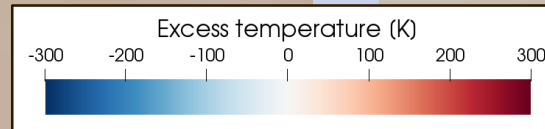
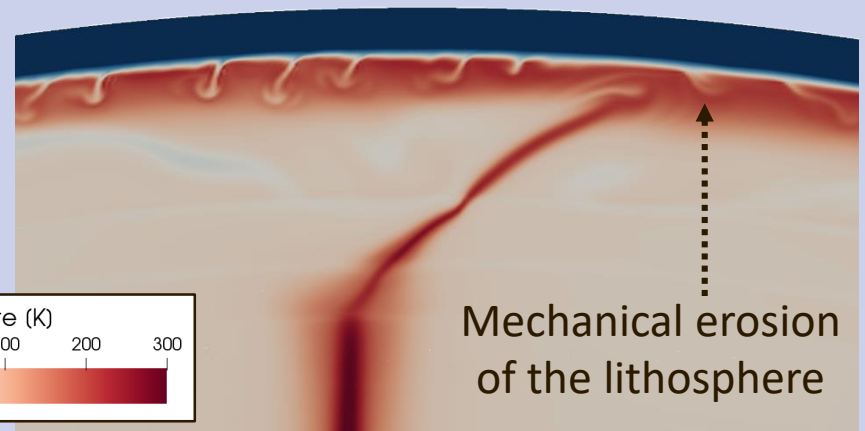
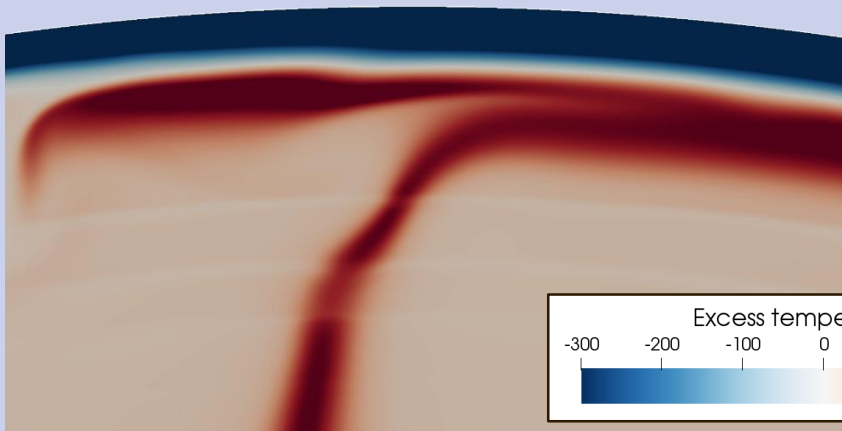
Lower mantle

- * Diffusion creep is dominant deformation mechanism
- * Grain growth is dominant, and depends on time spent in lower mantle

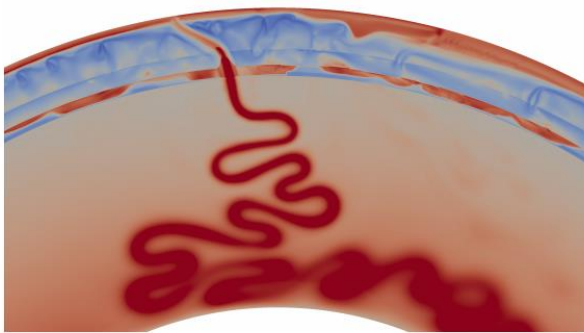
HOW GRAIN SIZE AFFECTS FLOW

Simple (diffusion creep) rheology

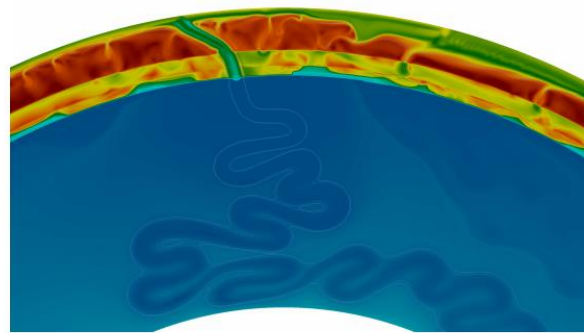
Grain size dependent rheology



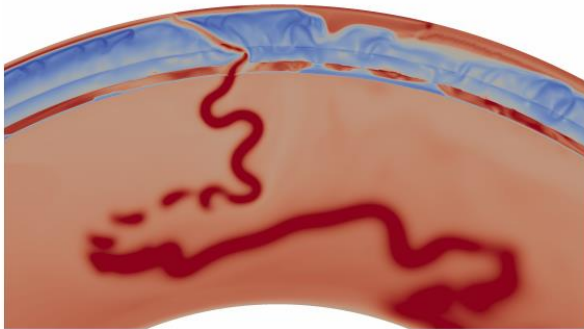
GRAIN SIZE EVOLUTION IN SLABS



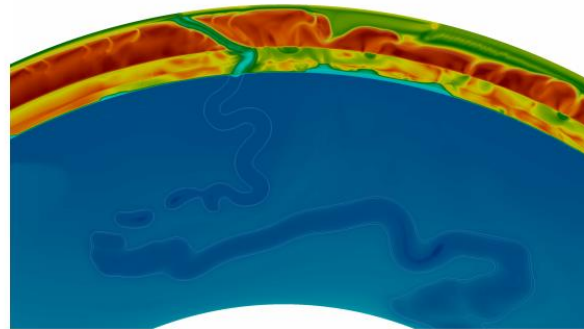
(c) Evolving grain size, LM $V_{diff} = 2e-6$



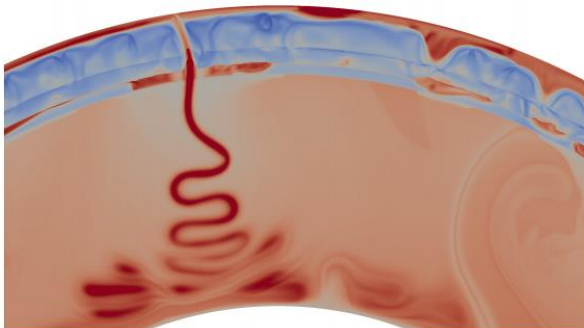
(d) Evolving grain size, LM $V_{diff} = 2e-6$



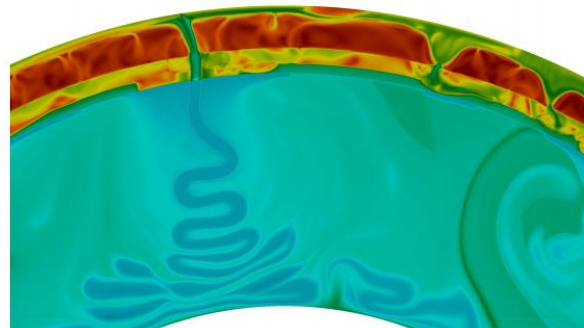
(e) Evolving grain size, LM $V_{diff} = 1.5e-6$



(f) Evolving grain size, LM $V_{diff} = 1.5e-6$



(g) Evolving grain size, faster LM growth

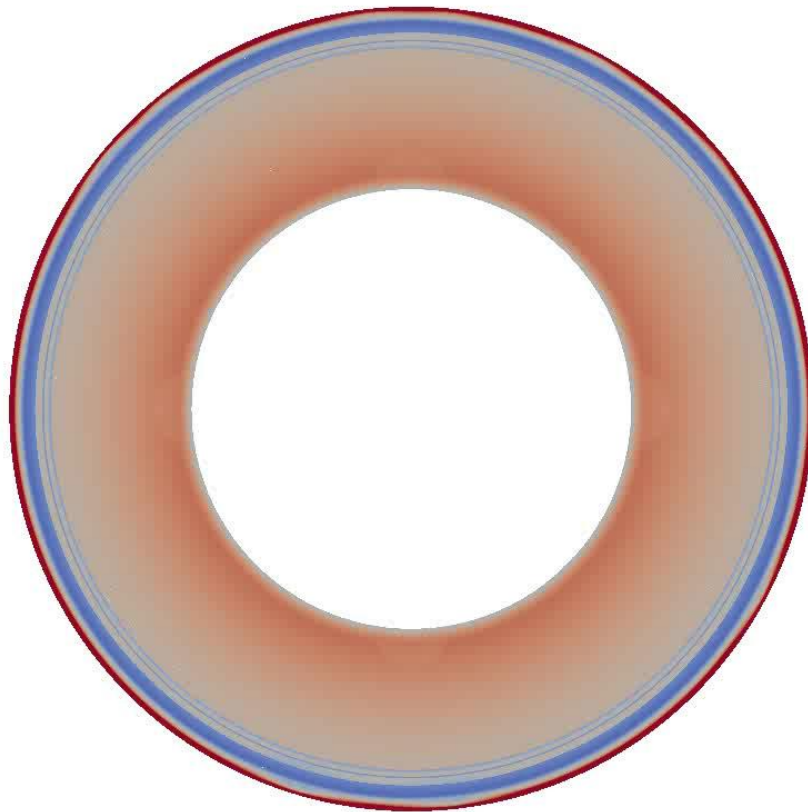


(h) Evolving grain size, faster LM growth

- * Small parameter variations change model behavior significantly
- * Qualitatively: bending instead of internal deformation

MODEL EVOLUTION

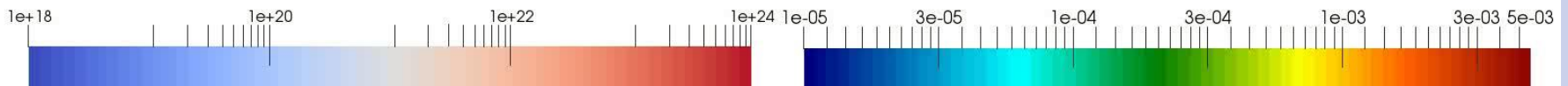
Time: 0 Ma



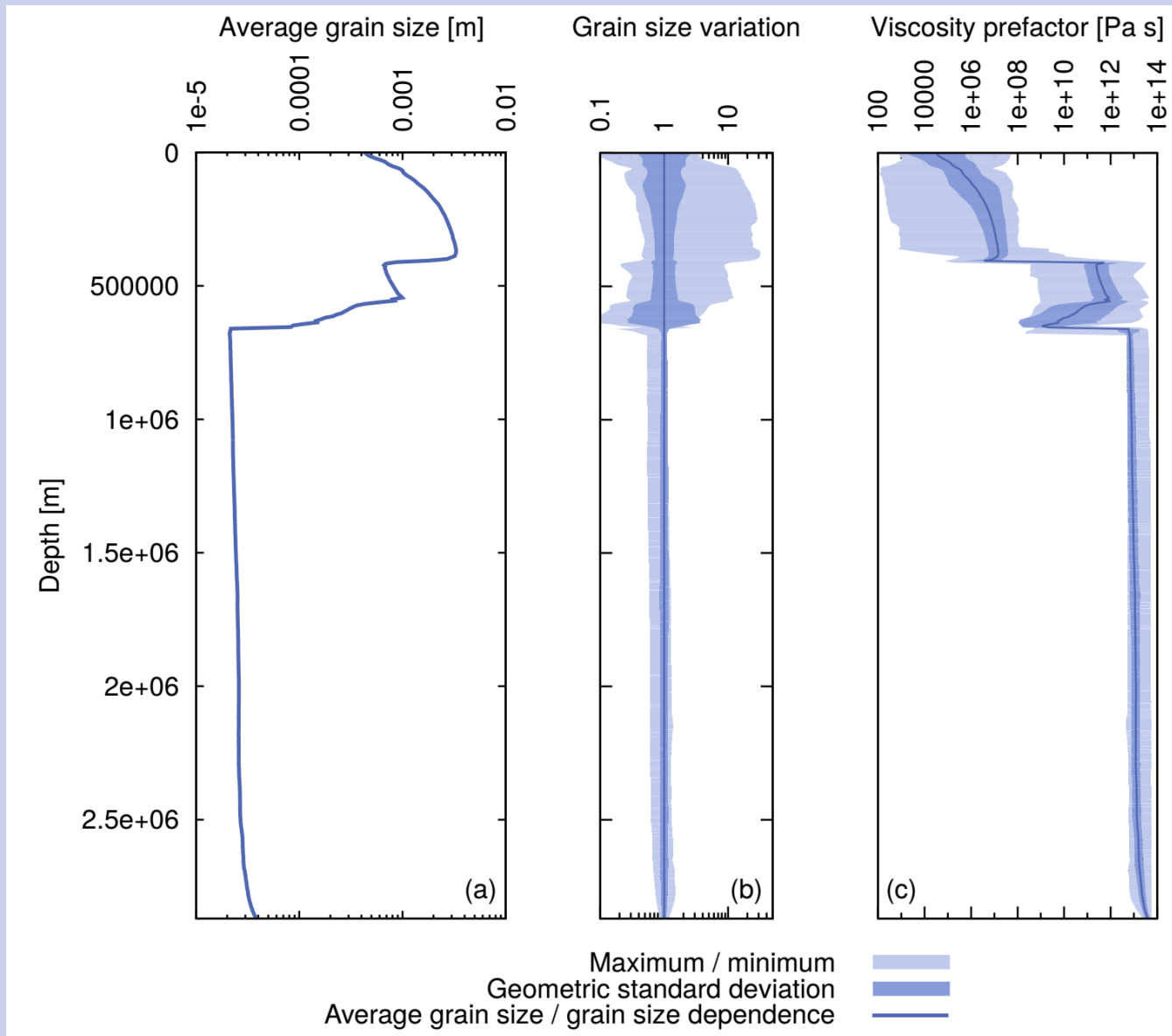
Viscosity (Pa s)



Grain size (m)



INFLUENCE OF GRAIN SIZE ON VISCOSITY



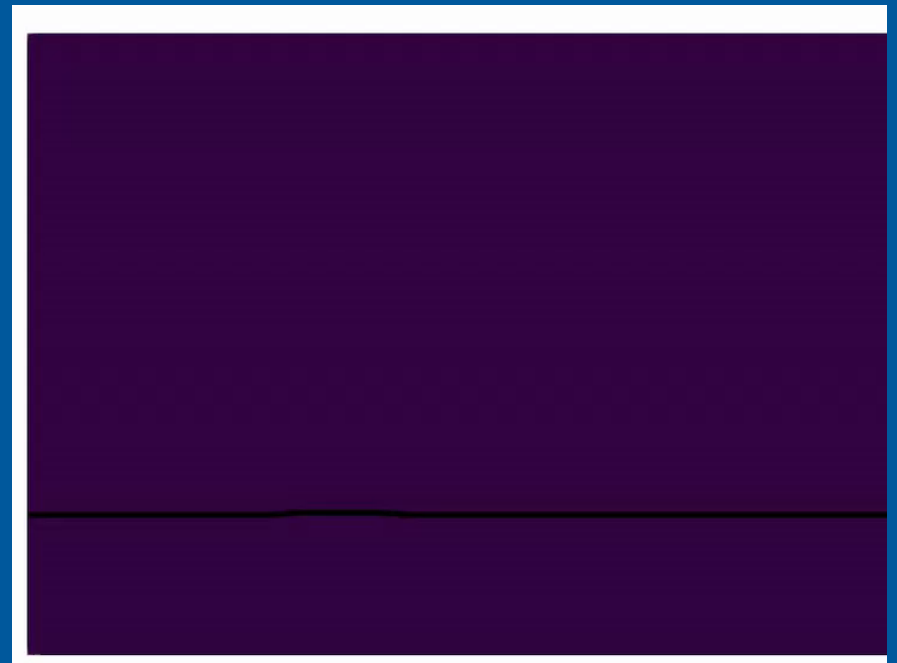
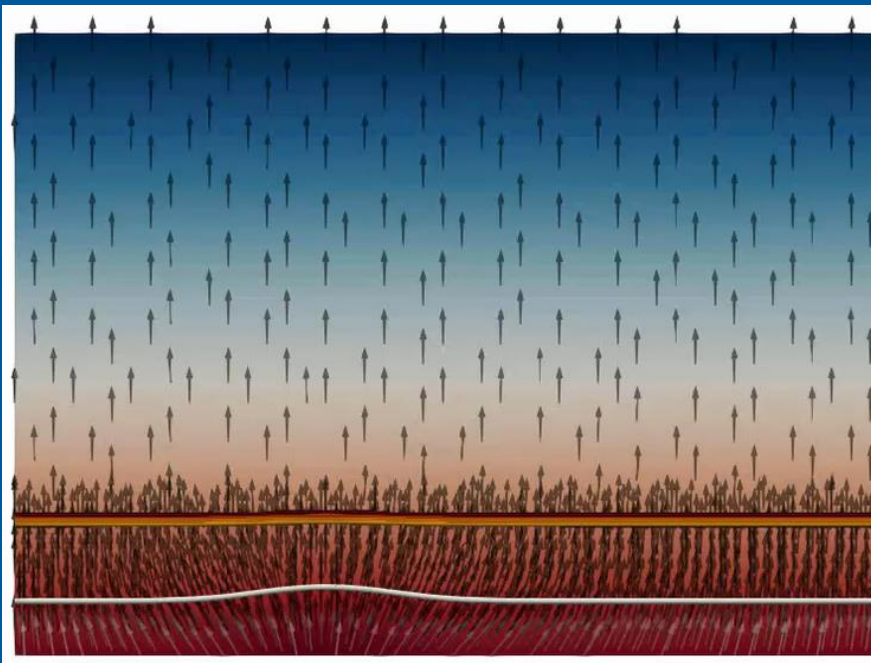
CONCLUSIONS



- * Dynamically evolving grain size in mantle convection models leads to high lateral viscosity contrasts and strong shear localization
- * In the lower mantle, viscosity may depend on how long ago material has crossed phase transitions
- * Viscosity at the edges of thermal plumes is lower than within, despite lower temperatures
- * Results qualitative, but grain size is a crucial control
- * Better constraints on grain growth and parameters in viscosity laws are needed

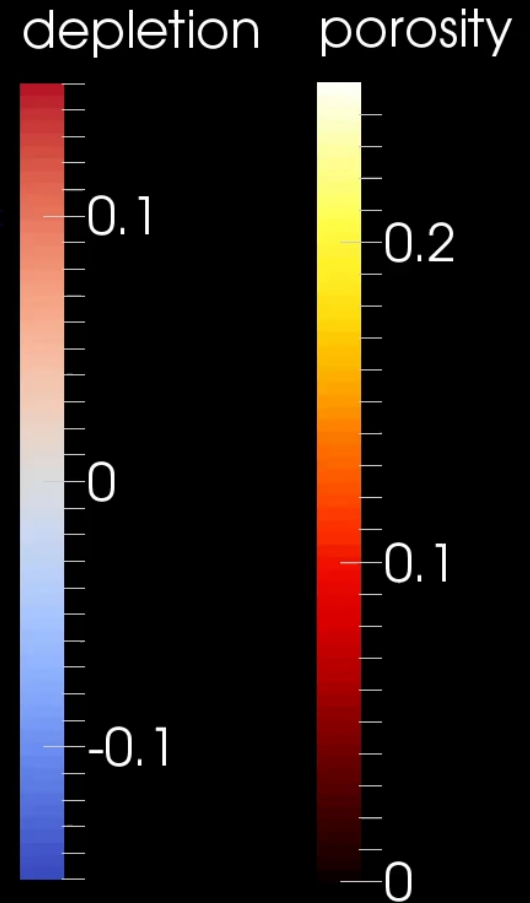
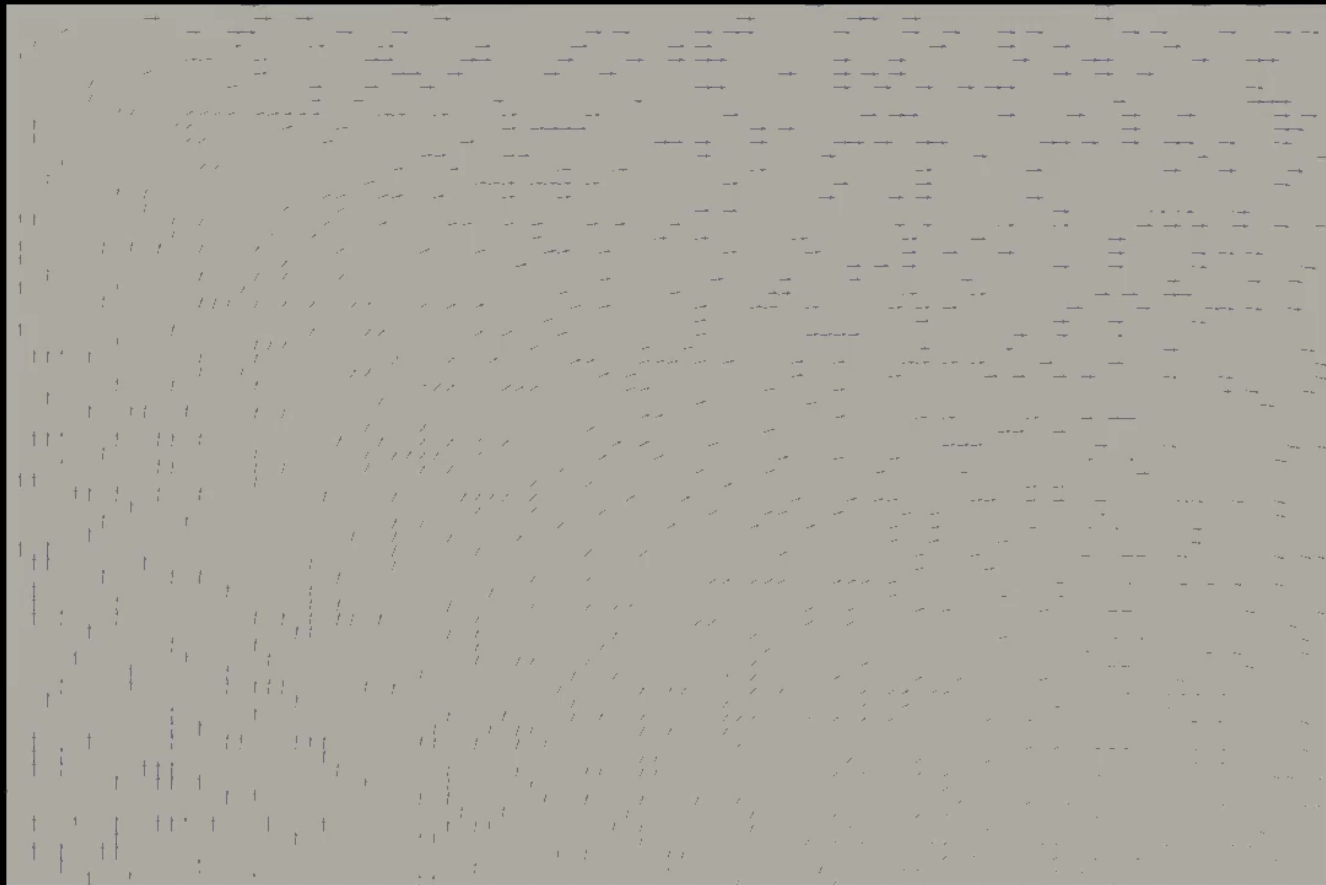
HETEROGENEITIES CAUSED BY MANTLE MELTING

Implications for ULVZs

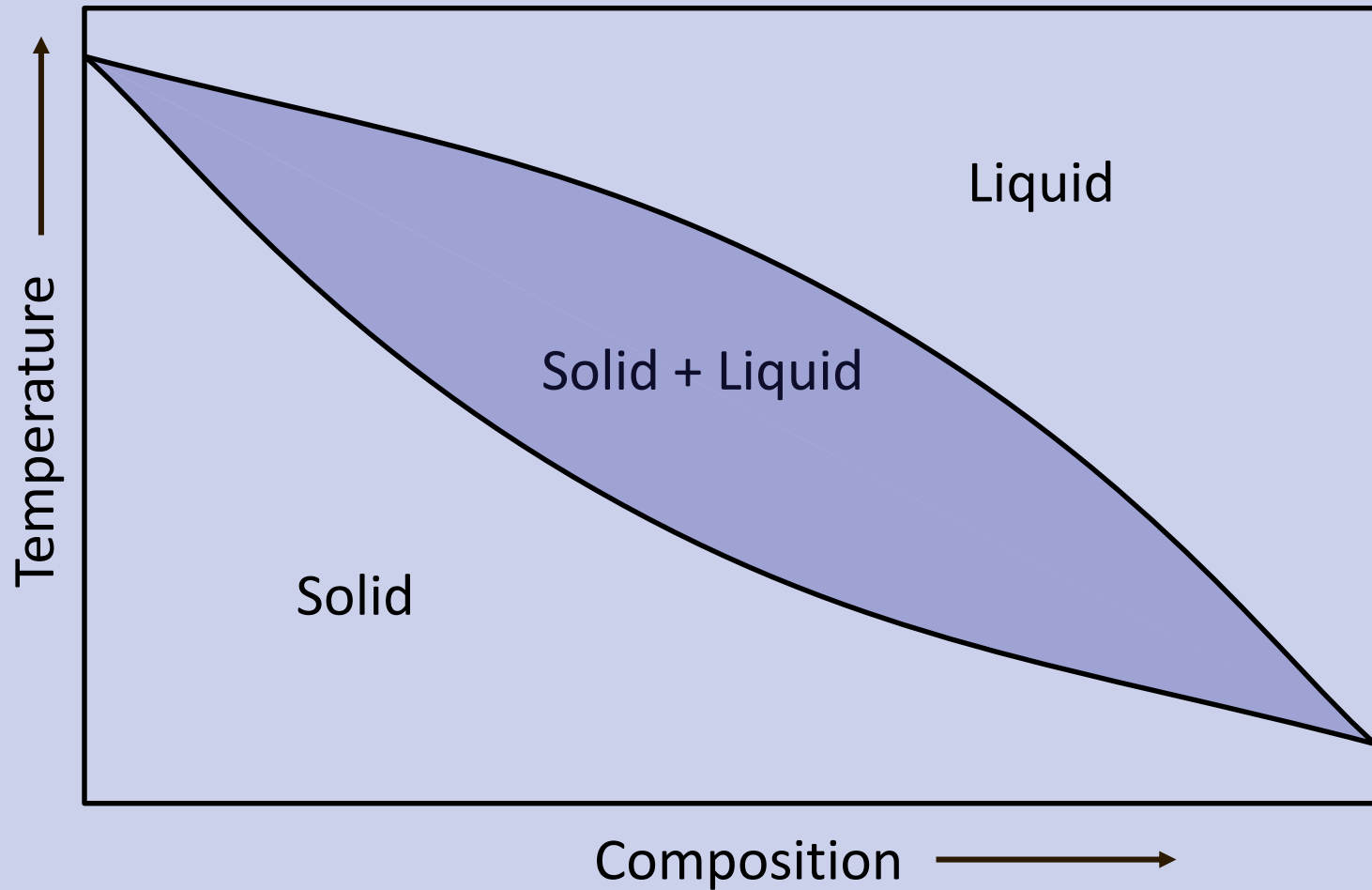


Work with R. Myhill, R. Gassmüller, S. Cottaar

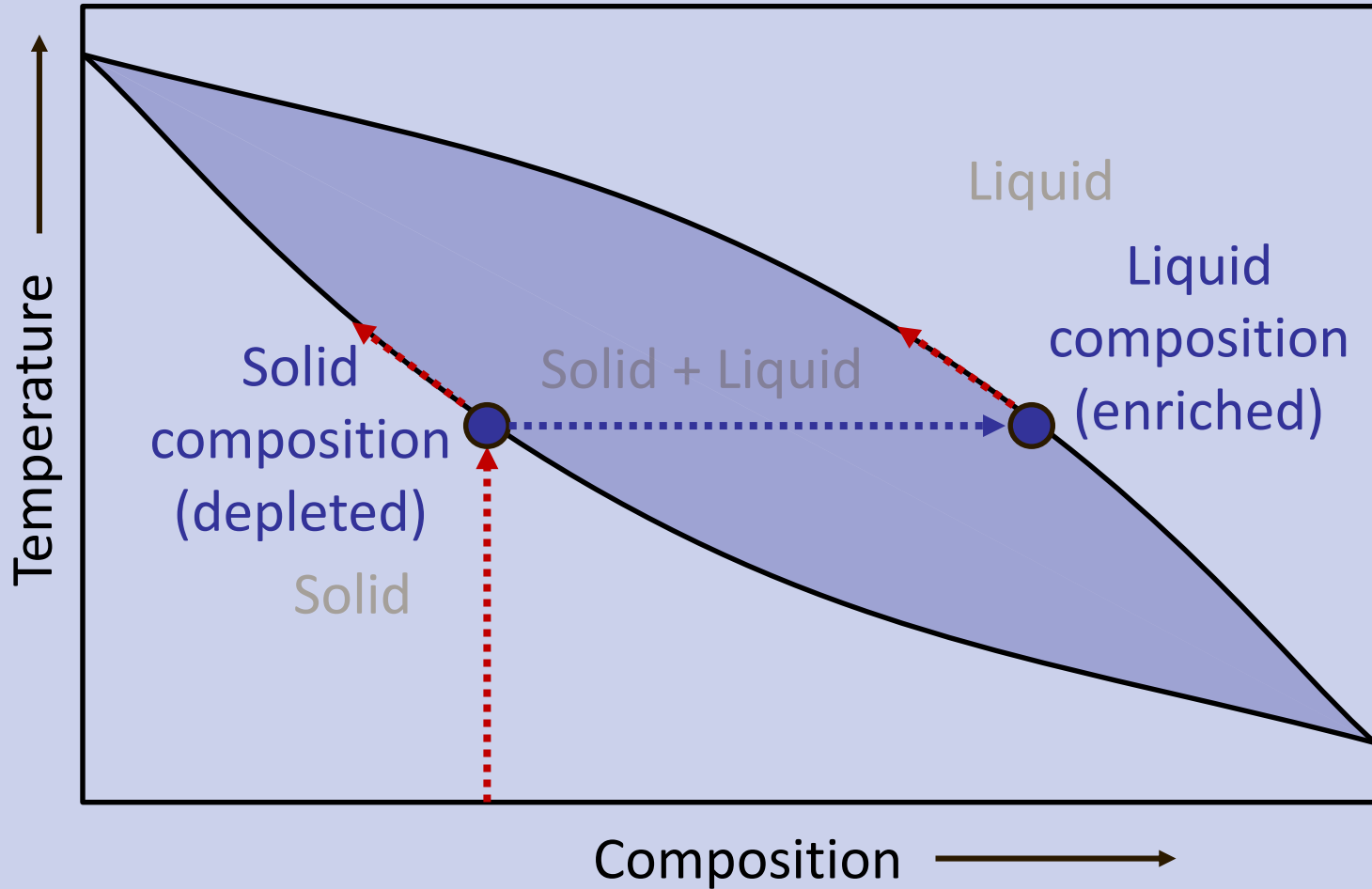
HETEROGENEITY: MID-OCEAN RIDGE



SIMPLE MANTLE MELTING MODEL

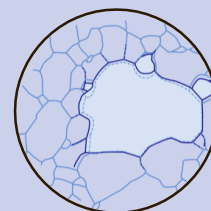
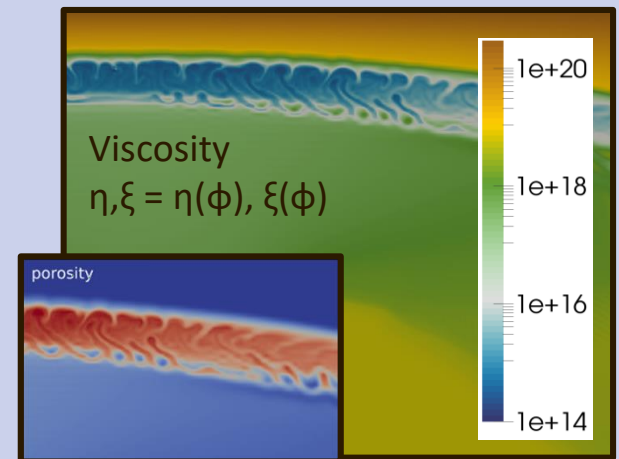
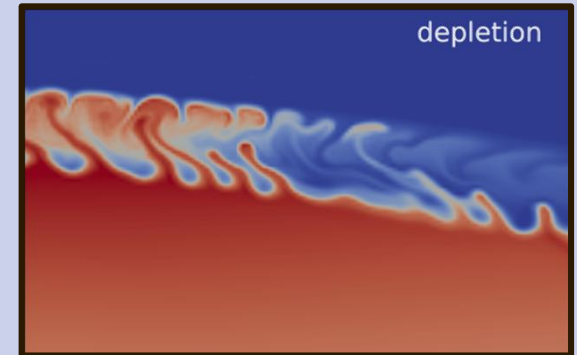


SIMPLE MANTLE MELTING MODEL



HETEROGENEITY: MID-OCEAN RIDGE

- * Melting, melt transport and freezing of melt introduce chemical heterogeneities.
- * Partially molten material is weaker than solid rock.
- * The presence of melt can make grain growth faster.



INFLUENCE ON GLOBAL CONVECTION

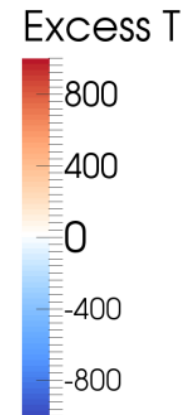
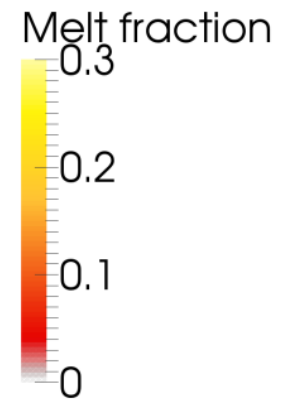
No melt migration



Time: 0.00e+00 years



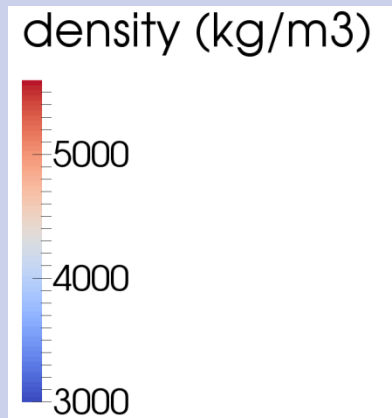
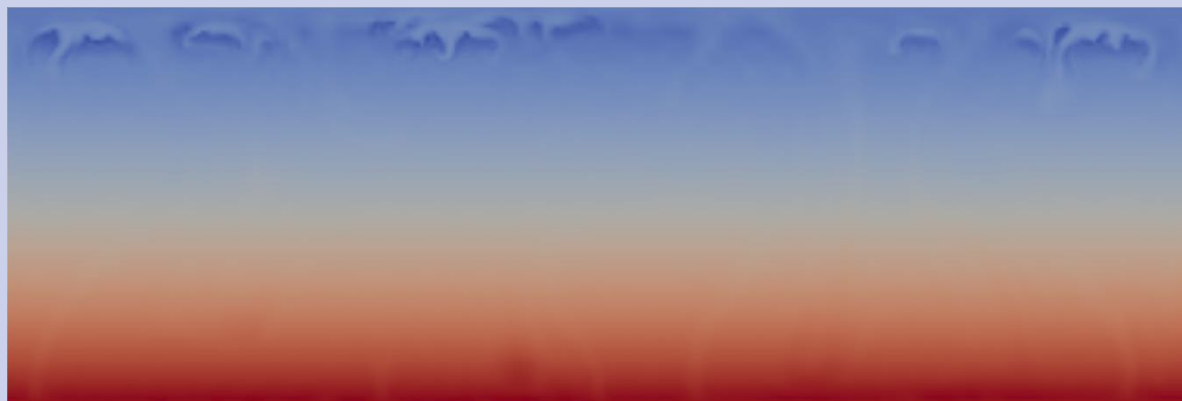
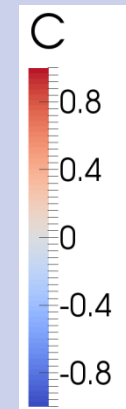
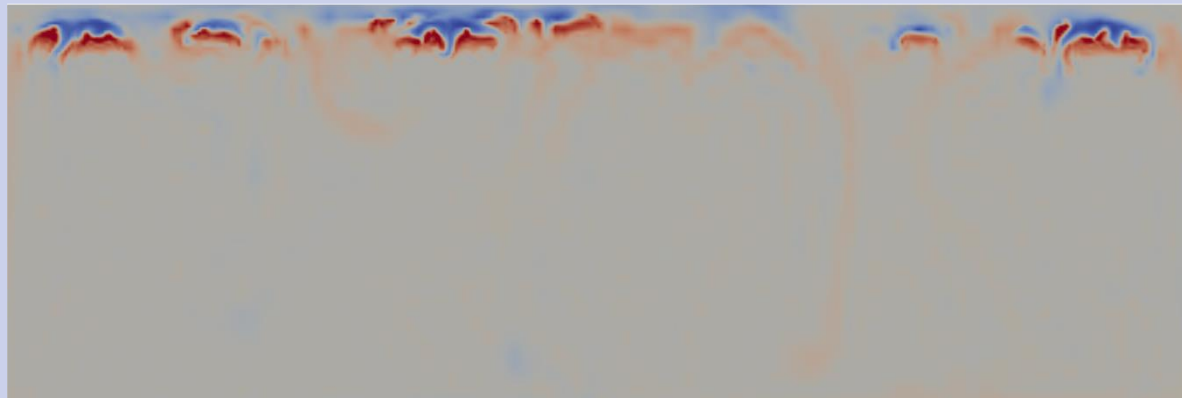
With melt migration



GLOBAL CONVECTION: DENSITY

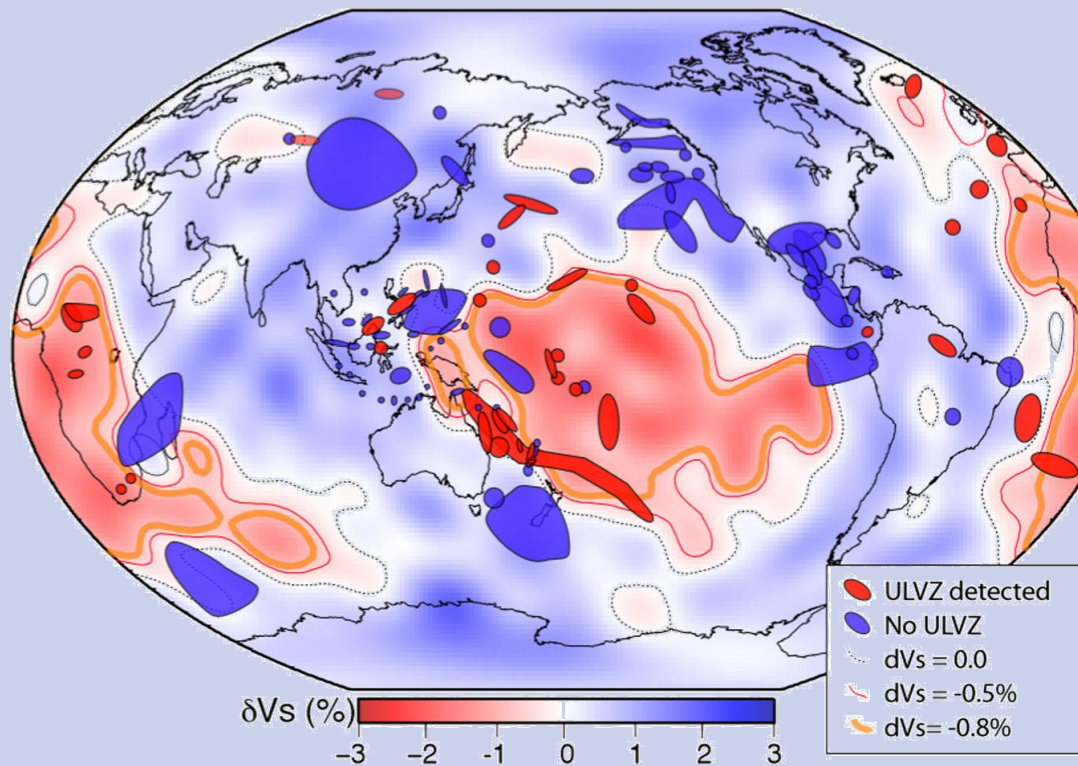
Crystallized melt (enriched material) is denser,

Depleted material is less dense: $\rho_s = \rho_0 + C \Delta\rho$



ULVZS

The lowermost mantle:



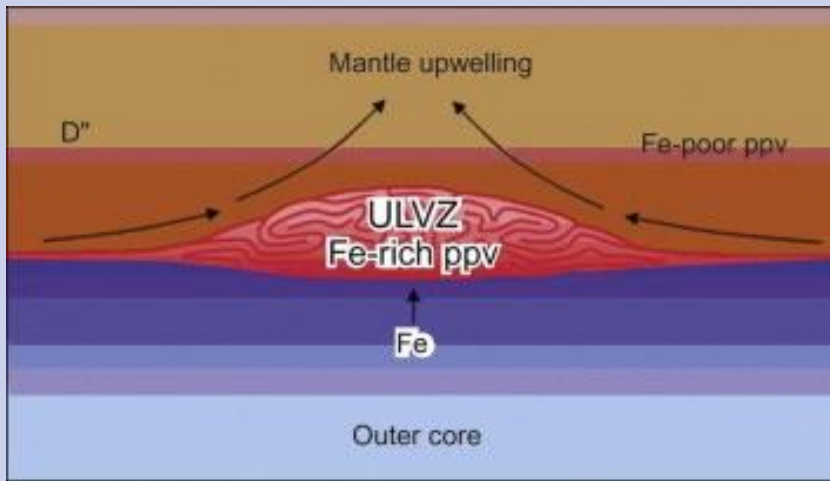
Observations:

- * Thin patches just above the core-mantle boundary
- * Velocity reductions of up to 30%
- * Located at the edges of LLSVPs and/or at the base of plume conduits
- * large aspect ratio, (100s-1000 km wide; 10-30 km thick)

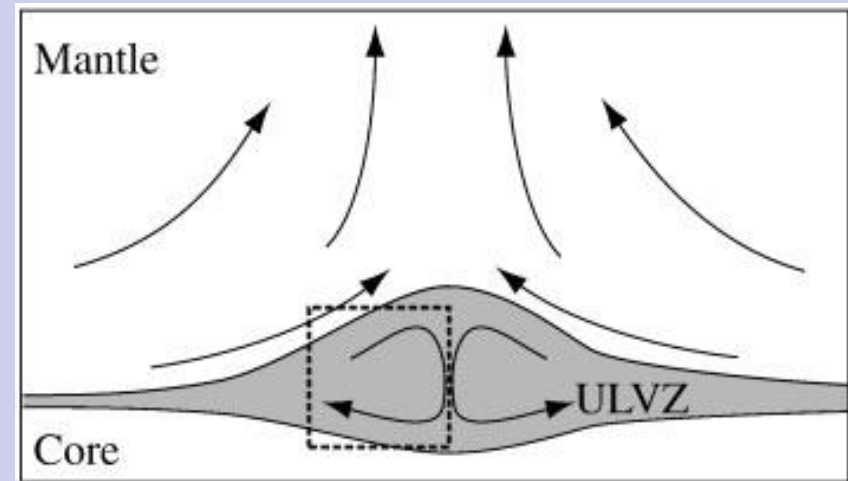
From McNamara, 2019

CAUSE OF VELOCITY REDUCTION

Compositional: Fe enrichment



Thermal: Partially molten

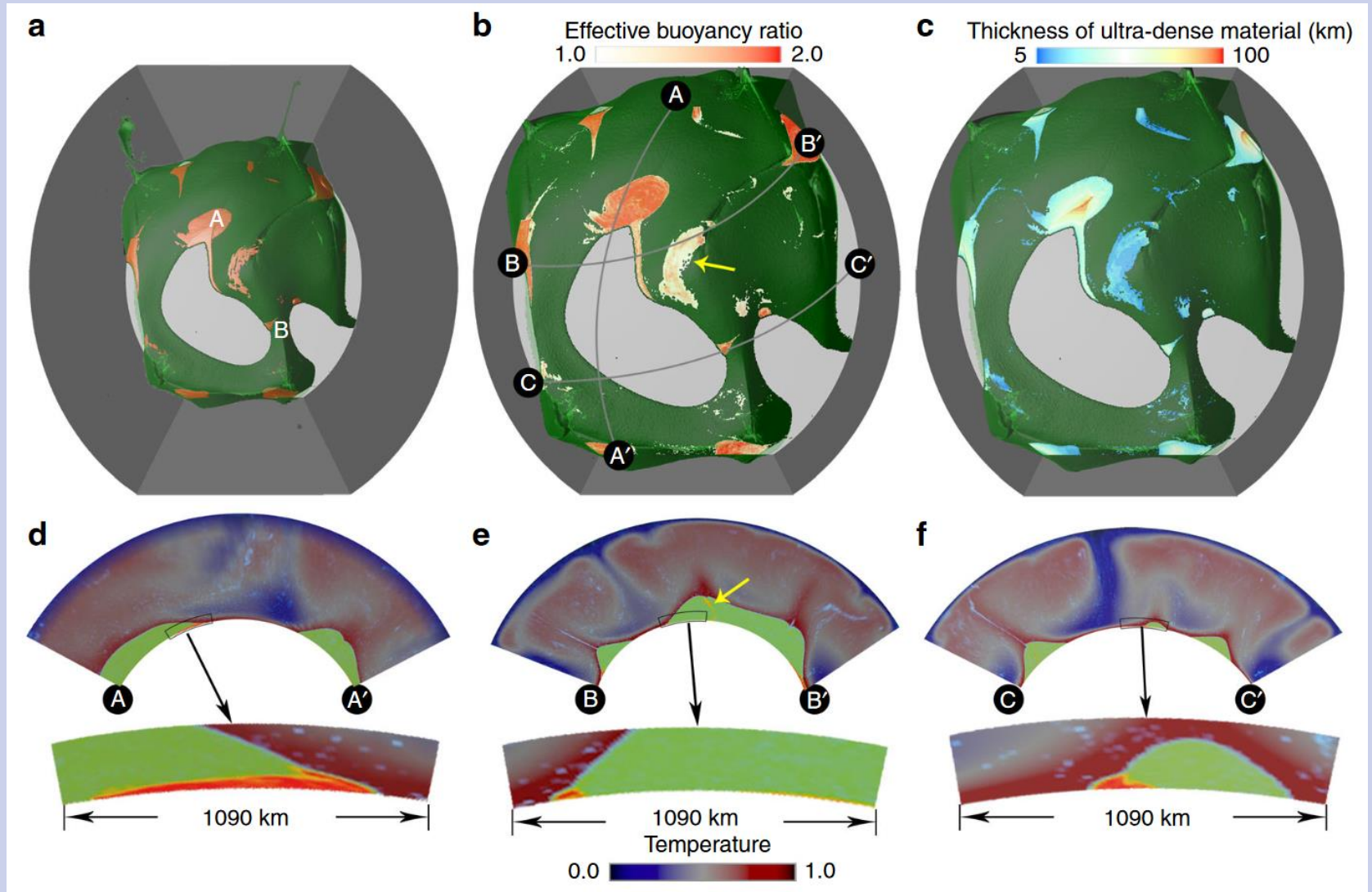


Hernlund & Jellinek, 2010

Both of the above

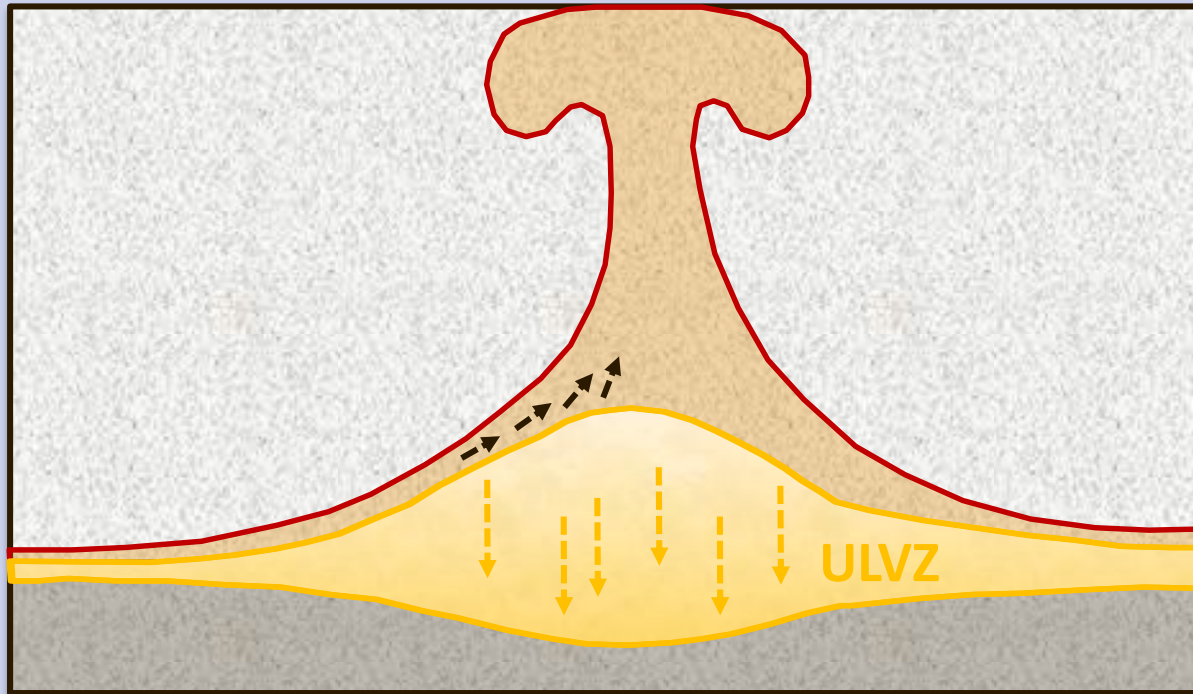
- Fe-enrichment can melt more easily
- Partial melt will be Fe-enriched

HYPOTHESIS: IRON ENRICHMENT



HYPOTHESIS: PARTIAL MELT

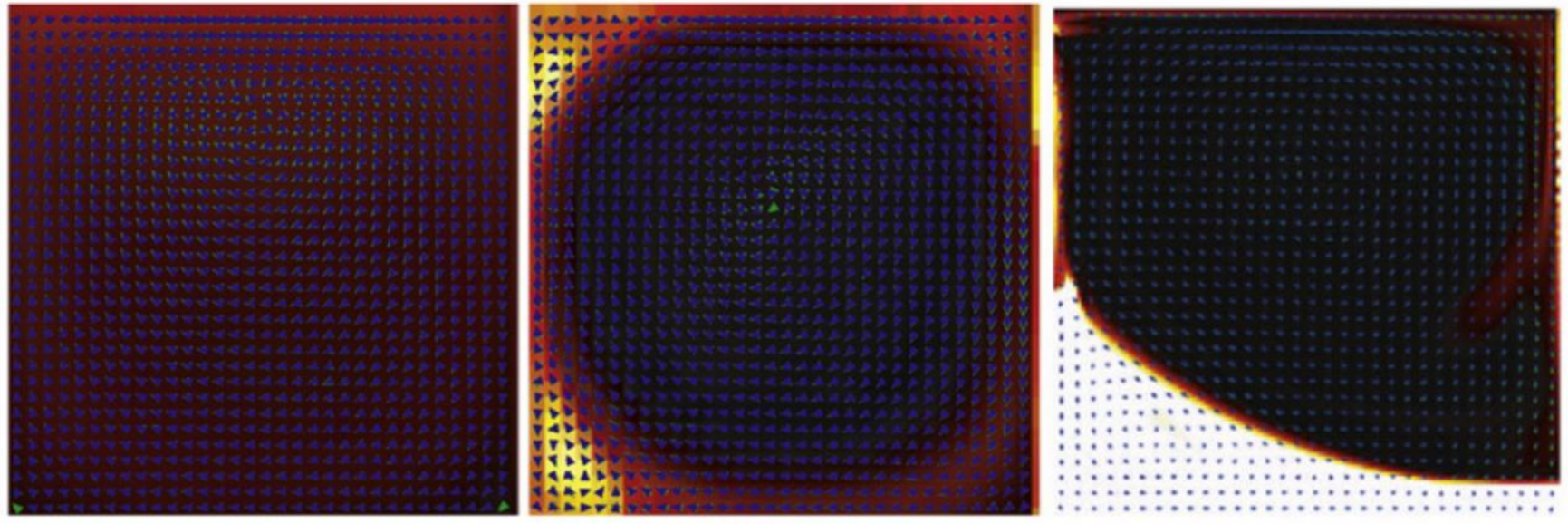
ULVZs contain partial melt which is constrained to a thin layer above the core-mantle boundary



- Viscous drag at the base of plumes introduces upwards flow
- Melt is dense and segregates downwards

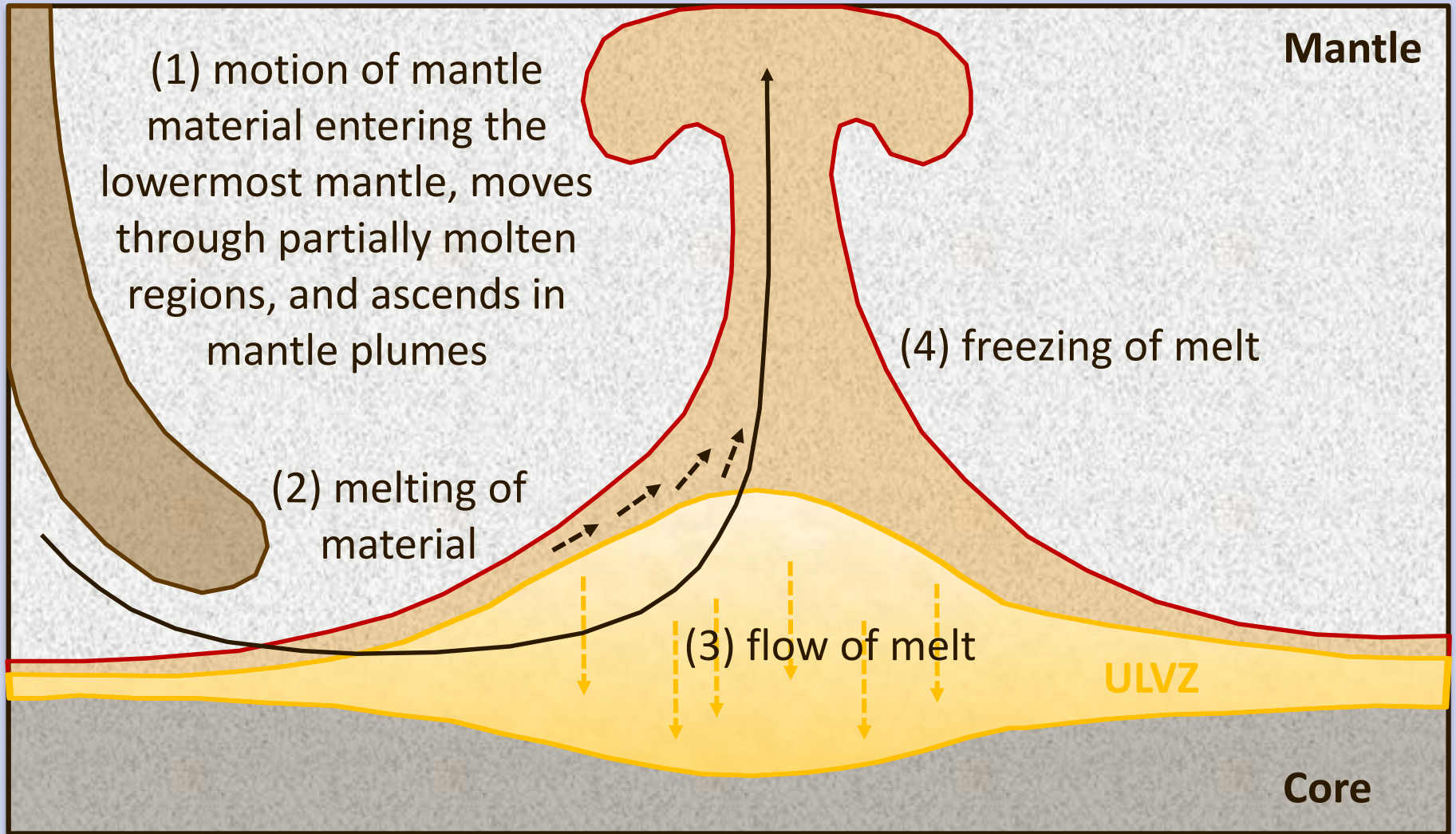
EXISTING MODELS

← Matrix Stress-Driven Separation Gravity-Driven Separation →



J.W. Hernlund, A.M. Jellinek /
Earth and Planetary Science
Letters 296 (2010) 1–8

IMPORTANT PROCESSES



MELTING MODEL

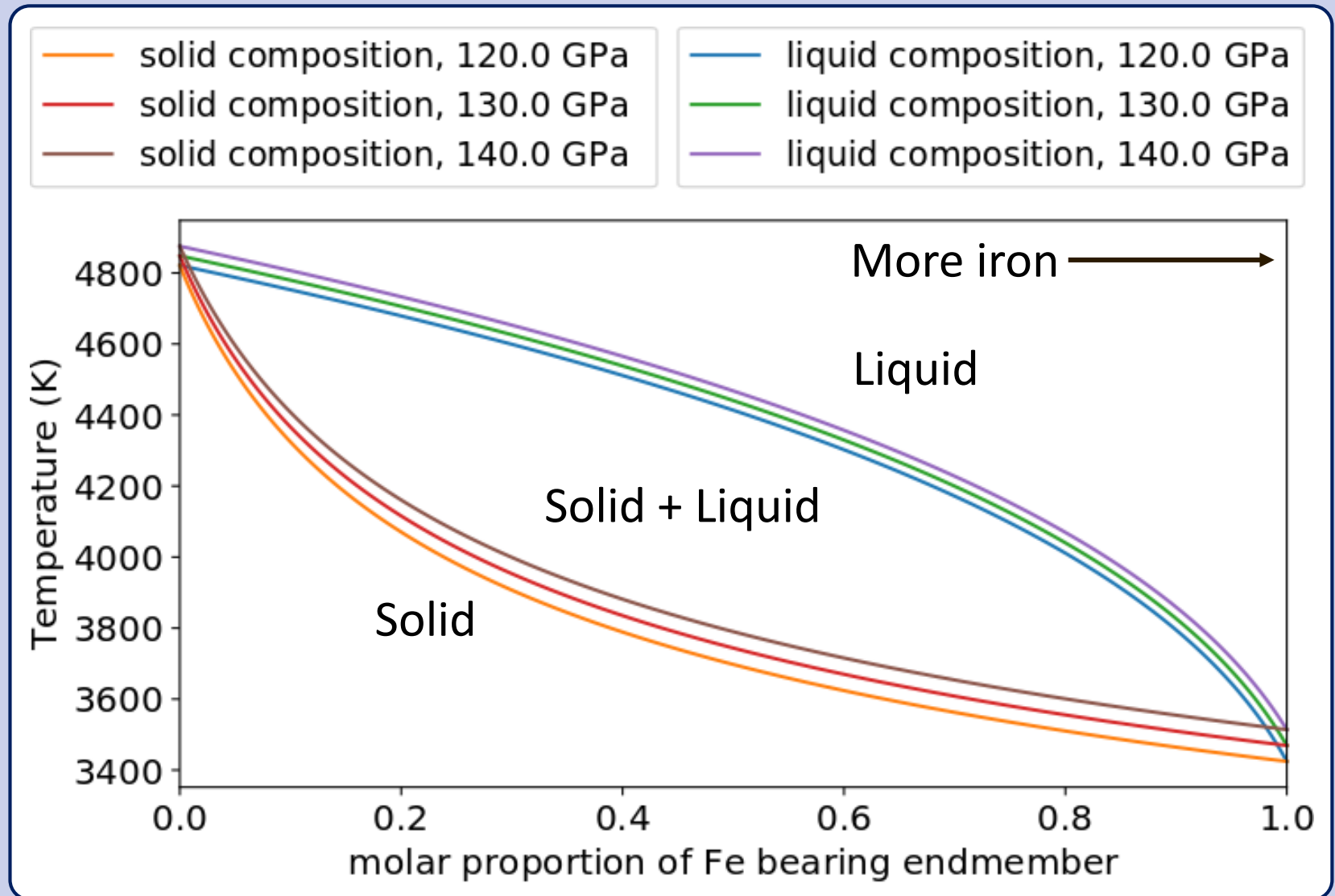


Figure and Modified melting model: R. Myhill

EQUATIONS: MAGMA/MANTLE DYNAMICS

Mass conservation

$$\frac{\partial}{\partial t} [\rho_f \phi] + \nabla \cdot [\rho_f \phi \mathbf{u}_f] = \Gamma$$

$$\frac{\partial}{\partial t} [\rho_s (1 - \phi)] + \nabla \cdot [\rho_s (1 - \phi) \mathbf{u}_s] = -\Gamma$$

Solid and fluid mass are conserved.

The difference
between solid
and melt velocity

depends on
the
permeability

and pressure
gradients in
the melt.

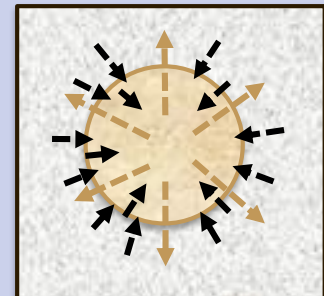
Momentum conservation

$$\phi (\mathbf{u}_f - \mathbf{u}_s) = -K_D (\nabla p_f - \rho_f \mathbf{g})$$

$$-\nabla \cdot \left[2\eta^* \left(\varepsilon(\mathbf{u}_s) - \frac{1}{3}(\nabla \cdot \mathbf{u}_s) \mathbf{1} \right) + \xi^* (\nabla \cdot \mathbf{u}_s) \mathbf{1} \right] + \nabla p_f = \bar{\rho} \mathbf{g}$$

In addition to being sheared...

the solid can also compact
and dilate as melt flows in
and out.



EQUATIONS: MAGMA/MANTLE DYNAMICS

Mass conservation

$$\frac{\partial}{\partial t} [\rho_f \phi] + \nabla \cdot [\rho_f \phi \mathbf{u}_f] = \Gamma$$

$$\frac{\partial}{\partial t} [\rho_s (1 - \phi)] + \nabla \cdot [\rho_s (1 - \phi) \mathbf{u}_s] = -\Gamma$$

Momentum conservation

$$\phi (\mathbf{u}_f - \mathbf{u}_s) = -K_D (\nabla p_f - \rho_f \mathbf{g})$$

$$-\nabla \cdot \left[2\eta^* \left(\varepsilon(\mathbf{u}_s) - \frac{1}{3} (\nabla \cdot \mathbf{u}_s) \mathbf{1} \right) + \xi^* (\nabla \cdot \mathbf{u}_s) \mathbf{1} \right] + \nabla p_f = \bar{\rho} \mathbf{g}$$

Energy conservation

$$\rho C_p \left(\frac{\partial T}{\partial t} + \mathbf{u} \cdot \nabla T \right) - \nabla \cdot k \nabla T = \dots \text{ (source terms)}$$

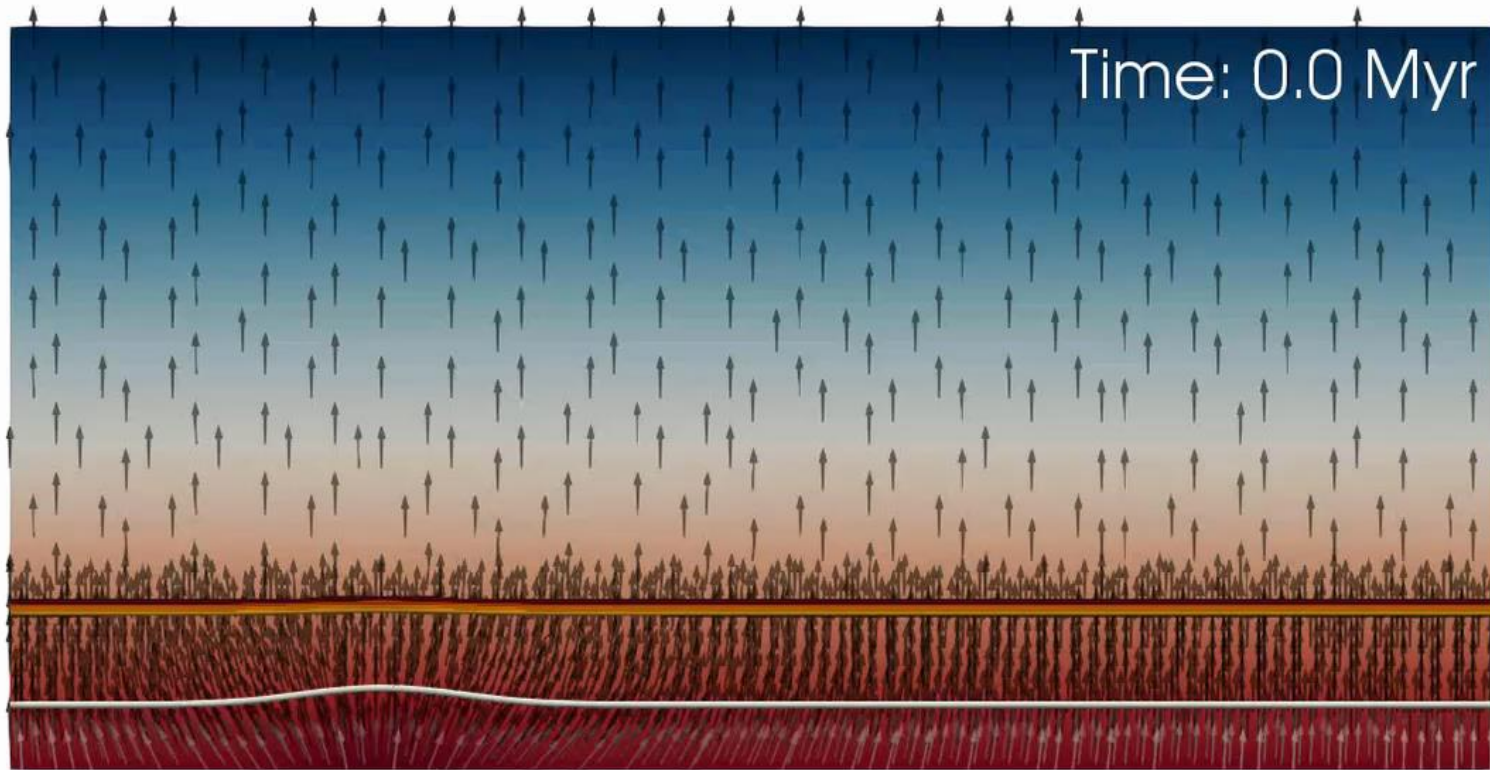
Chemical composition (n equations)

$$\frac{\partial \mathbf{c}(t)}{\partial t} + \mathbf{u} \cdot \nabla \mathbf{c}(t) = q(\mathbf{c}(t))$$

$\mathbf{u}_{s,f}$ solid, fluid velocity
 ϕ porosity
 p_f fluid pressure
 p_c compaction pressure
 $\rho_{s,f}$ density
 \mathbf{g} gravity
 Γ melting rate

HETEROGENEITY: LOWERMOST MANTLE

Time: 0.0 Myr



Temperature (K)

3400 3500 3600 3700 3800 3900 4000 4100 4200 4300 4400 4500



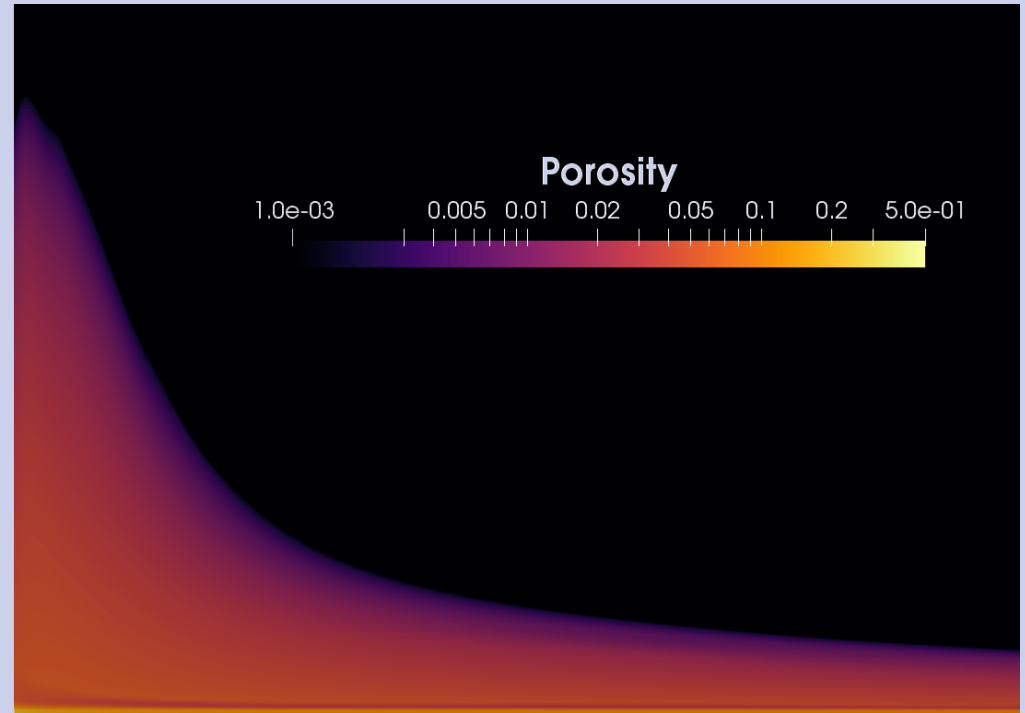
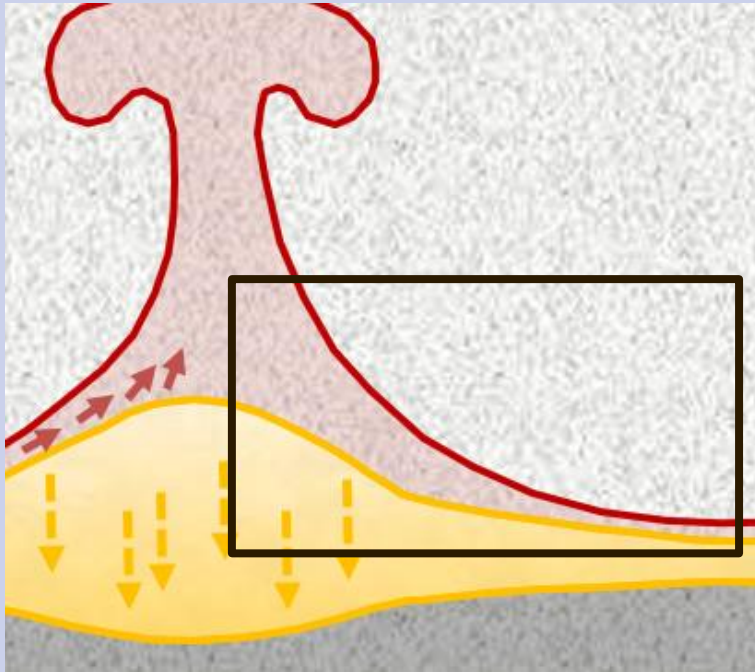
Melt volume fraction

1.0e-03 0.002 0.005 0.01 0.02 0.05 1.0e-01

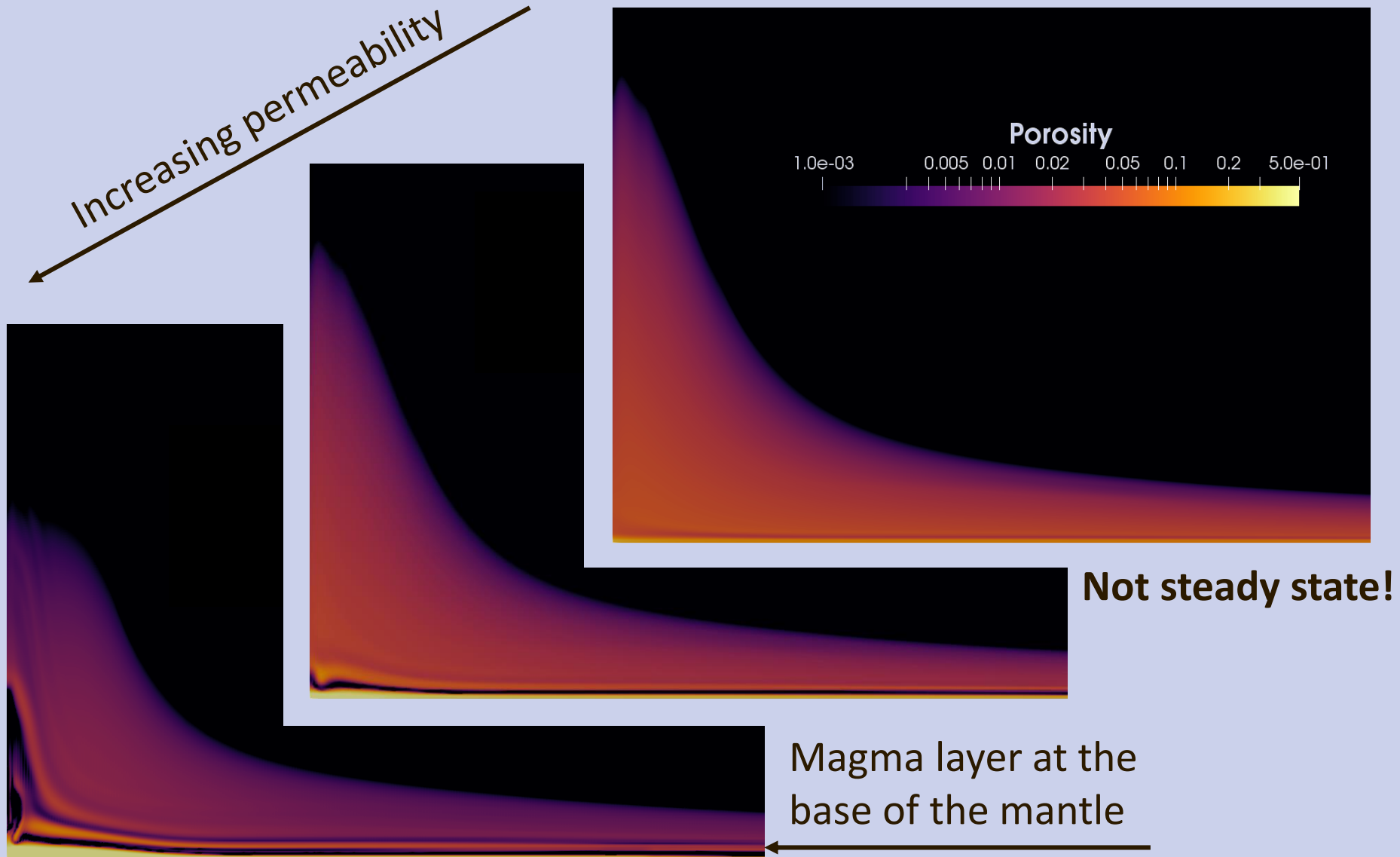


PRELIMINARY RESULTS

Geodynamic model



PRELIMINARY RESULTS



CONCLUSIONS



- * Mantle melting influences mantle heterogeneity by:
 - Changing mantle viscosity
 - Introducing chemical heterogeneities
 - Influencing grain growth

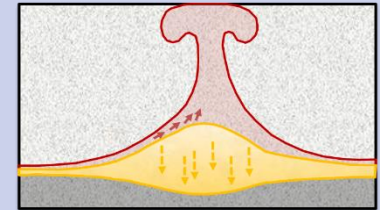
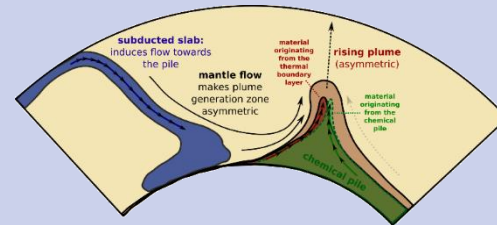
- * May even be important in the lower mantle:
potential explanation for ULVZs

I AM STARTING A GROUP...

...at University of Florida:


- * 2 postdoc positions
- * funding for 1 PhD student

Contact me: juliane.dannberg@ufl.edu



Juliane Dannberg

Home Research CV Publications Talks on the web KlarText Award



Assistant Professor
UF | Department of Geological Sciences
UNIVERSITY of FLORIDA

Email: juliane.dannberg@ufl.edu

 <https://orcid.org/0000-0003-0357-7115>

ASPECT

Advanced Solver for Problems in Earth's ConvecTion

